Structural transition, orientational order, and anomalous specific heat in a two-dimensional dimer crystal of core-softened particles

D. Pini,[1] T. Rovelli,[1] F. Mambretti,[2,3] and D. E. Galli[1]

[1]*Università degli Studi di Milano, Dipartimento di Fisica "Aldo Pontremoli", via Celoria 16, 20133 Milano, Italy*

[2]*Istituto Italiano di Tecnologia, via Melen 83, 16152 Genova, Italy*

[3]*Università degli Studi di Padova, Dipartimento di Fisica e Astronomia, via Marzolo 8, 35131 Padova, Italy*

(Received 19 December 2023; accepted 21 February 2024; published 25 March 2024)

Systems featuring hard-core–soft-shell repulsive pair potentials can form ordered phases, where particles organize themselves in aggregates with nontrivial geometries. The dimer crystal formed by one such potential, namely, the hard-core plus generalized exponential model of order 4, has been recently investigated, revealing a low-temperature structural phase transition, with the onset of nematic ordering of the dimers. In the present work, we aim to characterize this phase transition via a mean-field theory, by which a detailed analysis of the low-temperature properties of the system is carried out under quadrupole approximation. We determine the transition temperature and identify its order parameter, highlighting the link between the structural transition and the nematic ordering of the system. The first-order character of the transition is established and supported by the Landau expansion of the free energy in powers of the order parameter. The theory is subsequently generalized to take into account lattice vibrations and dimer length fluctuations. Finally, we provide an explanation for the anomalous behavior displayed by the specific heat in the vanishing-temperature limit, which is also supported by Monte Carlo simulations.

DOI: 10.1103/PhysRevE.109.034128

I. INTRODUCTION

In the soft-matter field, the effective interactions between complex molecules can generate phases which look highly different from those formed by their atomic constituents [1]. Soft materials are indeed made by units (much larger than atoms but also much smaller than the overall system size) which are sometimes found to form nontrivial structures, even in presence of purely pairwise forces.

An important class of interactions for which this occurs are the purely repulsive, yet bounded potentials belonging to the so-called $Q^{\pm}$ class [2], whose Fourier transform changes sign and reaches a negative absolute minimum at a nonvanishing wave vector k_m. For this kind of interactions, the very soft character of the shell repulsion acts in such a way that the overlap energy cost is almost independent of the mutual distance of the particles. Particles may then find preferable to self-organize into domains made up of overlapping particles separated by relatively large gaps, so that the interactions between particles belonging to different domains is very weak [3]. As a consequence, at low temperature or high density these interactions favor a transition from the fluid to a cluster crystal, whose lattice constant is determined by the interaction itself, and is then essentially state-independent [4,5].

The phenomenology is further enriched by combining this bounded repulsion with a hard-core, singular wall at shorter distance, resulting in potentials of the hard-core–soft-shell type, which serve as abstract models for the effective interactions in several systems, from colloids to polymers [6–12]. Unlike bounded potentials, which lead to structureless, point-like aggregates, such interactions can give rise to complex geometries, largely different from the usual close packing of spheres. Several of these nontrivial structures spontaneously present clusters, stripes, or rings [13–16].

In such a framework, we recently investigated the cluster phases of one-dimensional (1D) soft rods [17] and two-dimensional (2D) soft disks [18] interacting via purely repulsive potentials. In particular, in Ref. [18] we considered a specific instance of hard-core–soft-shell interaction, namely, the hard-core plus generalized exponential model of order 4 (HCGEM4) whose functional form is given in Sec. II, at a density such that clusters consist of just two particles at contact, resulting in a crystal of interacting dimers. We focused on the case in which the dimer length is much smaller than the lattice constant, so that each dimer is free to rotate with no steric hindrance from dimers on neighboring sites, and addressed the problem of determining the orientational order describing the lowest-energy configuration of the dimer crystal. To this end, we employed both Monte Carlo and Parallel Tempering numerical simulations at extremely low temperature, and a gradient minimization method of the potential energy of the system.

That study showed that, at zero or very low temperature, the dimers align along the same direction. With a slight lexical abuse, we shall refer to such a configuration as a nematic state, even though we are aware that this term is generally used to designate orientational order in liquid crystals which, unlike the system considered here, are not in a crystal state.

Rather than the kind of ordering *per se*, the more interesting result is the fact that, as was previously reported for a similar system of particles interacting via a hard-core plus square-shoulder potential [13,14], such a nematic state is achieved at

the price of a deformation of the triangular lattice, which describes a 2D crystal of HCGEM4 dimers (or, more generally, clusters) in the absence of orientational order. Specifically, the dimers arrange on a less symmetrical centered rectangular lattice, obtained from the triangular lattice by making one of the sides of each of the triangles which tessellate the plane shorter than the other two, to turn them from equilateral to isosceles. For short dimers the extent of this deformation is very small, but nevertheless it is crucial to stabilize the nematic phase. In fact, requiring artificially that the lattice remains triangular would lead to a very different kind of orientational order [18].

This result indicates that, besides the well-known fluid-crystal transition mentioned above, there should be another structural transition at lower temperature from the triangular to the centered rectangular lattice. Moreover, such a transition should be related to the one which leads from the orientationally disordered to the nematic phase, even though in principle the two transitions do not necessarily coincide.

The study of the structural transition and its relationship to the onset of the orientational order of the dimers is the subject of the present investigation. To this end, here we have focused on the HCGEM4 model at the same density considered in Ref. [18] and in the regime where the temperature is sufficiently low for it to form a dimer crystal, but the same analysis could be carried out for any hard-core plus $Q^{\pm}$ potential in the density and temperature range appropriate for dimer formation.

After introducing the model potential and briefly recalling the main features of clustering in the GEM4 and related interactions in Sec. II, we introduce a mean-field approach to describe the system in Sec. III. Specifically, in Sec. III A we develop a general formulation of the theory, which is then simplified by introducing the quadrupole approximation in Sec. III B. This treatment allows one to obtain the Helmholtz free energy and the probability distribution of the dimer orientation, and naturally leads to the identification of the order parameter of the structural transition, expressing the extent of the deviation of the crystal structure from the triangular lattice. Moreover, we find that the structural and orientational transitions actually coincide: formally, this is expressed by the explicit dependence of the nematic order parameter on the structural order parameter.

The main features of the transition resulting from the present description are considered in Sec. III C, where a Landau expansion of the free energy is performed as a function of the structural order parameter, and it is found that its form is characteristic of a first-order transition. The expression of the transition temperature and the discontinuities of the order parameter and of the specific heat at constant volume at the transition are also determined to leading order in the dimer length.

Since the above results are based on the minimization of the mean-field Helmholtz free energy in a certain subset of all possible lattice deformations, in Sec. III D it is shown that the minimum remains stable even when all deformations compatible with the given density are considered. Subsequently, in Sec. III E the theory is expanded to account for thermal fluctuations in the positions of the lattice sites and of the dimer length. This adds no new information about the qualitative features of the transition, but nevertheless it is important to do so, given that in the system at hand those degrees of freedom are actually present.

Even though an extended comparison between the predictions of the mean-field approach and the simulation results is deferred to a future publication, here we have also performed some Monte Carlo simulations to evaluate the specific heat at temperatures much lower than the transition temperature. The simulation method is described in Sec. IV.

In Sec. V the results obtained via the numerical minimization of the mean-field Helmholtz free energy are presented and discussed. These include the transition temperature for different dimer lengths and the temperature dependence of the structural and nematic order parameters and of the specific heat. Special attention is paid to the explanation of the behavior of the specific heat at very low temperature, where both theory and simulation display a deviation from the limit expected on the basis of the equipartition of energy.

Finally, in Sec. VI we summarize the main results of the study and draw our conclusions. In order not to make the exposition too cumbersome, some technical points considered in Secs. III and V have been derived in detail in Appendices A–D.

II. MODEL POTENTIAL

The pair interaction considered in this work, following Ref. [18], has a soft part which is a generalized exponential model of order 4 (GEM4) [4,5,19]

$$w(r) = \varepsilon \exp[-(r/R)^4], \tag{1}$$

as a function of the interparticle distance r. R and ε set the range and strength of this potential, respectively. We then add a repulsive hard-core of diameter 2δ, obtaining the HCGEM4 potential $\phi_{\mathrm{HCGEM4}}(r)$ given by

$$\phi_{\mathrm{HCGEM4}}(r) = \begin{cases} \infty & r < 2\delta, \\ \varepsilon \exp[-(r/R)^4] & r \geqslant 2\delta. \end{cases} \tag{2}$$

In the following, 2δ will range from $0.05\,R$ to $0.25\,R$, corresponding to a shell-to-core ratio equal to 20 and 4 respectively (note that in Ref. [18] the hard-core diameter was denoted by δ).

As extensively discussed in previous works [4,5], the GEM4 potential belongs to the $Q^{\pm}$ class mentioned in Sec. I, its Fourier transform reaching the absolute minimum at $k_m = 5.09618\,R^{-1}$. $Q^{\pm}$ interactions tend to display spontaneous density modulations, which at low temperature or high density manifest themselves as inhomogeneous, periodic phases, with a periodicity dictated by k_m [5].

At variance with atomic crystals, where each lattice site is occupied by a single particle and a change in the number density ρ necessarily entails a change in the lattice spacing, in these systems more particles pile up at the same lattice site and a change in ρ is achieved by changing the site occupation number n_c, while leaving the lattice spacing nearly unchanged. This implies a linear relation between ρ and n_c, which for the triangular lattice reads

$$\rho = \frac{\sqrt{3}\,k_m^2}{8\pi^2} n_c. \tag{3}$$

In this study, as in Ref. [18], we have considered the system at fixed density $\rho = 1.13971R^{-2}$, obtained from Eq. (3) by setting $n_c = 2$ and $k_m = 5.09679R^{-1}$. The latter value is slightly different from that of the GEM4 potential reported above, because it corresponds to the "regularized" HCGEM4 interaction used in the simulations, see Sec. IV, whereby the hard-core repulsion is replaced by a step of finite amplitude, and the step function is included in the evaluation of the Fourier transform. Either choice of k_m is acceptable, because in both cases ρ belongs to the density interval where, at low temperature, a monodisperse dimer phase is formed.

In fact, in the low-temperature regime thermal motion is unable to redistribute particles among lattice sites, and n_c is bound to assume integer values. As a consequence, densities which according to Eq. (3) would correspond to nearly integer n_c are obtained by keeping n_c integer, and slightly changing the lattice constant with respect to the optimal value. Instead, densities corresponding to noninteger n_c lying midway between two consecutive integers, say n and $n+1$, are actually obtained by having phases with $n_c = n$ and $n_c = n+1$ coexist with each other [20,21]. The latter instance is not relevant here, where we are interested in the case of dimer formation, such that $n_c = 2$.

For the HCGEM4 potential, dimers are not point-like objects, since the hard-core repulsion prevents the two disks on each site from fully overlapping. Hence, the orientation of each dimer becomes a relevant degree of freedom.

III. MEAN-FIELD THEORY

A. General formulation

We consider N particles mutually interacting via the HCGEM4 potential of Eq. (2), arranged as an assembly of $N/2$ dimers on a 2D crystal lattice. In this section, as well as in Secs. III B–III D, we shall not take into account thermal oscillations of either the lattice sites or the dimer length. The latter then coincides with the hard-core diameter 2δ of the potential at all temperatures. The position of the dimer particles at site $i = 1 \dots N/2$ can be expressed as

$$\mathbf{x}_{i,\sigma} = \mathbf{R}_i + \sigma\boldsymbol{\delta}_i, \tag{4}$$

where $\mathbf{R}_i$ is the position of the i site, $\sigma = \pm 1$ is the index identifying the two particles of the dimer, and $\boldsymbol{\delta}_i$ is the vector of length δ connecting the center of the dimer with, say, particle 1. A given configuration is then identified by the angles $\vartheta_1 \dots \vartheta_{N/2}$, $0 \leqslant \vartheta_i < 2\pi$ for each i, which specify the orientation of the dimers with respect to a fixed direction, that we identify with the x axis. We remark that, since the two particles in a dimer are distinguishable, the angles ϑ_i and $\vartheta_i + \pi$ represent different configurations, although the two are of course degenerate. The potential energy of the system is

$$U = \frac{1}{2}\sum_{i\neq j,\sigma,\sigma'} w(\mathbf{R}_i - \mathbf{R}_j + \sigma\boldsymbol{\delta}_i - \sigma'\boldsymbol{\delta}_j) + \frac{N}{2}w(2\delta), \tag{5}$$

where $w(r)$ is the GEM4 potential of Eq. (1). The first and second term of Eq. (5) refer respectively to the interdimer interaction between the dimers at different sites, and to the intradimer interaction between the particles within the same dimer.

The Helmholtz free energy of the system consists of the sum of its kinetic term K and its configurational term F. The former is not relevant to the phase behavior and, in the present case where the $N/2$ angles ϑ_i are the only degrees of freedom, amounts to $K = k_{\mathrm{B}}TN/4$, where T is the temperature, and k_{B} is Boltzmann constant. We now focus on the configurational Helmholtz free energy F, which will be studied by a mean-field approximation. This approximation may be formulated in several ways, but the most straightforward one is based on the application of Gibbs' variational principle to the probability distribution of the dimer configurations. According to Gibbs' principle, if $P(\vartheta_1 \dots \vartheta_{N/2})$ is a (normalized) probability distribution and we denote by $\langle f\rangle$ the corresponding average of a generic function $f(\vartheta_1 \dots \vartheta_{N/2})$ such that

$$\langle f\rangle = \int_0^{2\pi} d\vartheta_1 \dots \int_0^{2\pi} d\vartheta_{N/2}\, P(\vartheta_1 \dots \vartheta_{N/2}) f(\vartheta_1 \dots \vartheta_{N/2}), \tag{6}$$

then the equilibrium distribution P_0 is that which minimizes the functional $\Psi[P]$ given by

$$\Psi[P] = \langle U\rangle + k_{\mathrm{B}}T\,\langle \ln P\rangle, \tag{7}$$

By evaluating $\Psi[P]$ at P_0, the configurational Helmholtz free energy F is obtained.

The mean-field approximation amounts to representing $P(\vartheta_1 \dots \vartheta_{N/2})$ as the product of $N/2$ independent one-dimer contributions by setting

$$P(\vartheta_1 \dots \vartheta_{N/2}) = p(\vartheta_1) \times \cdots \times p(\vartheta_{N/2}). \tag{8}$$

Clearly, Eq. (8) implies the neglect of correlations between dimer orientations. Besides this limit inherent to the mean-field approximation, we also note that, since $p(\vartheta)$ is assumed to be the same for all dimers, such an *ansatz* is unable to describe any kind of orientational order different from the nematic one. The rationale for considering only nematic order is that, as stated in Sec. I, our former study [18] showed that a nematic phase is indeed the preferred state at $T = 0$. It is then natural to assume that such a phase will still occur at low, but nonvanishing temperature, even though this does not rule out *a priori* the possibility that also other, more complex ordered phases might appear, which are not accounted for by the present theory.

By adopting the factorization of Eq. (8), the entropic term of Eq. (7) is straightforwardly expressed in terms of $p(\vartheta)$ as

$$\langle \ln P\rangle = \frac{N}{2}\int_0^{2\pi} d\vartheta\, p(\vartheta)\ln p(\vartheta), \tag{9}$$

whereas for the energetic term we find

$$\langle U\rangle = \frac{1}{2}\int_0^{2\pi} d\vartheta \int_0^{2\pi} d\vartheta' \left\{ \sum_{i\neq j,\sigma,\sigma'} w[\mathbf{R}_i - \mathbf{R}_j + \sigma\boldsymbol{\delta}(\vartheta) - \sigma'\boldsymbol{\delta}(\vartheta')] p(\vartheta)\, p(\vartheta') \right\} + \frac{N}{2}w(2\delta). \tag{10}$$

To disentangle the dependence on the dimer orientation from the interaction potential $w(r)$, it is useful to express Eq. (10) in Fourier space by introducing the Fourier transform $\widetilde{w}(q)$ of the interaction

$$\widetilde{w}(q) = \int d\mathbf{r}\, e^{-i\mathbf{q}\cdot\mathbf{r}} w(r). \tag{11}$$

Equation (10) then becomes

$$\langle U\rangle = \frac{N}{v}\sum_{\mathbf{k}}\langle\cos(\mathbf{k}\cdot\boldsymbol{\delta})\rangle^2\widetilde{w}(k) - N\int\frac{d\mathbf{q}}{(2\pi)^2} \langle\cos(\mathbf{q}\cdot\boldsymbol{\delta})\rangle^2\widetilde{w}(q) + \frac{N}{2}w(2\delta), \tag{12}$$

where v is the volume of the primitive cell, the sum runs over the vectors $\mathbf{k}$ of the reciprocal lattice, the integral is extended to the whole plane, and we have indicated by $\langle\ldots\rangle$ the averages over the dimer orientation according to the one-dimer probability distribution $p(\vartheta)$. The integral in Eq. (12) stems from the $i \neq j$ constraint in Eq. (10) and accounts for the fact that, even though in the mean-field approach different dimers are regarded as uncorrelated, the two particles within the same dimer should still be considered as (trivially) correlated, since the orientation of either particle is determined by that of the other. This can be appreciated in the limiting case of a crystal with a very large lattice constant, such that the interactions between dimers on different sites can be disregarded altogether. In this limit, the lattice constant of the reciprocal lattice becomes very small and in Eq. (12) the sum over $\mathbf{k}$ tends to the integral over $\mathbf{q}$, so that the two contributions cancel out, and $\langle U\rangle$ correctly reduces to the intradimer term $Nw(2\delta)/2$. Disregarding the integral would amount to adding to the intradimer energy a contribution in which the positions of the two particles would be taken as independent, which is clearly incorrect.

By adding up Eqs. (9) and (12) and setting $\beta = 1/(k_{\mathrm{B}}T)$, we obtain

$$\frac{\beta F}{N} = \frac{\beta}{v}\sum_{\mathbf{k}}\langle\cos(\mathbf{k}\cdot\boldsymbol{\delta})\rangle^2\widetilde{w}(k) - \beta\int\frac{d\mathbf{q}}{(2\pi)^2} \langle\cos(\mathbf{q}\cdot\boldsymbol{\delta})\rangle^2\widetilde{w}(q) + \frac{1}{2}\langle\ln p\rangle + \frac{\beta}{2}w(2\delta). \tag{13}$$

Following Gibbs' principle, the equilibrium distribution is determined by functional minimization of $\beta F/N$ given by Eq. (13) with respect to $p(\vartheta)$, i.e.,

$$\frac{\delta}{\delta p(\vartheta)}\left[\frac{\beta F}{N} - \zeta\int_0^{2\pi} d\vartheta\, p(\vartheta)\right] = 0, \tag{14}$$

where $\delta/\delta p(\vartheta)$ indicates functional differentiation, and ζ is a Lagrange multiplier to be determined by the normalization condition for $p(\vartheta)$.

If we set $c(\mathbf{q}) = \langle\cos(\mathbf{q}\cdot\boldsymbol{\delta})\rangle$, then the solution of Eq. (14) gives for the equilibrium distribution

$$p(\vartheta) = \frac{1}{Q}\exp\left[-\frac{4\beta}{v}\sum_{\mathbf{k}}c(\mathbf{k})\cos(\mathbf{k}\cdot\boldsymbol{\delta})\widetilde{w}(k) + 4\beta\int\frac{d\mathbf{q}}{(2\pi)^2}c(\mathbf{q})\cos(\mathbf{q}\cdot\boldsymbol{\delta})\widetilde{w}(q)\right], \tag{15}$$

where Q is the one-dimer partition function

$$Q = \int_0^{2\pi} d\vartheta\exp\left[-\frac{4\beta}{v}\sum_{\mathbf{k}}c(\mathbf{k})\cos(\mathbf{k}\cdot\boldsymbol{\delta})\widetilde{w}(k) + 4\beta\int\frac{d\mathbf{q}}{(2\pi)^2}c(\mathbf{q})\cos(\mathbf{q}\cdot\boldsymbol{\delta})\widetilde{w}(q)\right]. \tag{16}$$

Substitution of Eq. (15) into Eq. (13) gives

$$\frac{\beta F}{N} = -\frac{\beta}{v}\sum_{\mathbf{k}}c(\mathbf{k})^2\widetilde{w}(k) + \beta\int\frac{d\mathbf{q}}{(2\pi)^2}c(\mathbf{q})^2\widetilde{w}(q) + \frac{\beta}{2}w(2\delta) - \frac{1}{2}\ln Q, \tag{17}$$

with $c(\mathbf{q})$ to be determined by the self-consistency condition

$$c(\mathbf{q}) = \frac{1}{Q}\int_0^{2\pi} d\vartheta\cos(\mathbf{q}\cdot\boldsymbol{\delta}) \times\exp\left[-\frac{4\beta}{v}\sum_{\mathbf{k}}c(\mathbf{k})\cos(\mathbf{k}\cdot\boldsymbol{\delta})\widetilde{w}(k) + 4\beta\int\frac{d\mathbf{q}'}{(2\pi)^2}c(\mathbf{q}')\cos(\mathbf{q}'\cdot\boldsymbol{\delta})\widetilde{w}(q')\right]. \tag{18}$$

Equations (16)–(18) determine the mean-field Helmholtz free energy F of the dimer crystal for a given lattice. In the present situation in which the lattice has not been fixed beforehand and the crystal may undergo a structural transition, F must be also optimized with respect to the lattice itself. In general, for a 2D lattice four scalars would be needed, one for each component of the two primitive vectors. However, here we are considering the system at fixed density ρ, which fixes the cell volume at $v = 2/\rho$. Moreover, the x axis can be aligned with one of the primitive vectors with no loss of generality, leaving two independent scalars. These we identify with the lattice constant a and with a dimensionless parameter s such that $\cot\psi = a^2 s/v$, where ψ is the angle between the primitive vectors. We then set

$$\mathbf{A} = \begin{pmatrix} a & as \\ 0 & v/a \end{pmatrix} \quad \mathbf{B} = \frac{2\pi}{v}\begin{pmatrix} v/a & 0 \\ -as & a \end{pmatrix}, \tag{19}$$

where $\mathbf{A}$ is the matrix obtained by arranging the primitive lattice vectors into columns, and $\mathbf{B}$ is the corresponding matrix of the reciprocal lattice. The triangular lattice is identified by $a = a_0 = (2v/\sqrt{3})^{1/2}$, $s = 1/2$.

It is worthwhile pointing out that, according to Eqs. (15) and (18), the probability distribution of the dimer orientation $p(\vartheta)$ *cannot* be uniform, whatever the temperature. A constant $p(\vartheta)$ over the interval $(0, 2\pi)$ would yield

$$c(\mathbf{q}) \equiv \langle\cos(\mathbf{q}\cdot\boldsymbol{\delta})\rangle = J_0(q\delta), \tag{20}$$

where $J_0(x)$ is the Bessel function of order 0

$$J_0(x) = \frac{1}{2\pi}\int_0^{2\pi} d\vartheta\, e^{-ix\cos\vartheta}. \tag{21}$$

If Eq. (20) were a self-consistent solution of Eq. (18), then plugging it into Eq. (15) should give back $p(\vartheta) \equiv 1/(2\pi)$, i.e., the argument of the exponential in the rhs of Eq.(15) should

not depend on the direction of $\boldsymbol{\delta}$. That argument contains an integral I over $\mathbf{q}$,

$$I = \int \frac{d\mathbf{q}}{(2\pi)^2} \cos(\mathbf{q}\cdot\boldsymbol{\delta})\, J_0(q\delta)\widetilde{w}(q), \tag{22}$$

and a sum Σ over the reciprocal lattice vectors $\mathbf{k}$,

$$\Sigma = \sum_{\mathbf{k}} \cos(\mathbf{k}\cdot\boldsymbol{\delta})\, J_0(k\delta)\widetilde{w}(k). \tag{23}$$

The integral I is indeed isotropic, since it is the inverse Fourier transform of an isotropic function. However, this is not the case for the sum Σ, which *does* depend on the direction of $\boldsymbol{\delta}$, as can also be readily checked numerically.

The fact that $p(\vartheta)$ cannot be isotropic is perhaps not surprising: since the dimers themselves are not uniformly distributed, but lie instead on a crystal lattice, there is no reason why the field exerted on a given dimer by all the others should be independent of the direction. Such a scenario is different from that of liquid crystals for which, in their orientationally disordered state, all orientations are equivalent.

Having said so, two important remarks are in order: first, this situation does not prevent the possibility that, just as in liquid crystals, the system may have no macroscopic orientational order. Consider the case of the highly symmetric triangular lattice: even though $p(\vartheta)$ displays maxima for some preferred directions, the lattice invariance under rotations of 60° implies that, if the invariance is not spontaneously broken, those directions will add up to give no net orientational order.

Second, even though strictly speaking $p(\vartheta)$ is not uniform, in the absence of orientational order it may be *nearly* uniform, provided the dimer length 2δ is small compared to the lattice constant a. As stated above, a uniform $p(\vartheta)$ cannot be reconciled with the fact that the quantity Σ in Eq. (23) depends on ϑ, i.e., on the direction of $\boldsymbol{\delta}$. However, if we consider again the triangular lattice, that dependence is very weak. In fact, in a multipole expansion in which $\cos(\mathbf{k}\cdot\boldsymbol{\delta})$ in Eq. (23) is expanded in powers of its argument, both the second-order quadrupole and the fourth-order octupole terms are found to be actually isotropic. Specifically, we have

$$\sum_{\mathbf{k}\in\mathcal{T}} (\mathbf{k}\cdot\boldsymbol{\delta})^2 g(k) = \frac{1}{2}\,\delta^2 \sum_{\mathbf{k}\in\mathcal{T}} k^2 g(k), \tag{24}$$

$$\sum_{\mathbf{k}\in\mathcal{T}} (\mathbf{k}\cdot\boldsymbol{\delta})^4 g(k) = \frac{3}{8}\,\delta^4 \sum_{\mathbf{k}\in\mathcal{T}} k^4 g(k), \tag{25}$$

where $\mathcal{T}$ denotes the triangular lattice, and $g(k)$ is a generic spherically symmetric function such that the sums over $\mathbf{k}$ are convergent. The dependence on the direction of $\boldsymbol{\delta}$ appears only at order δ^6 or higher, i.e., from the esadecapole term on. For small δ, this is indeed a very small effect, and we expect that, in the absence of orientational order, the errors induced by regarding $p(\vartheta)$ as if it were uniform should be similarly small. In the next section we shall introduce such an approximation.

B. Quadrupole approximation

The theory described in Sec. III A has two drawbacks: first, it hinges on the self-consistency condition of Eq. (18) for $c(\mathbf{q})$. This equation is rather involved, and requires a fully numerical solution. Second, it does not lead to a clear identification of the order parameter of the transition. To simplify the treatment and make the underlying physics more perspicuous, in the following we shall not be concerned with the solution of Eq. (18), but shall consider instead a simplified formulation of the theory, based on the quadrupole approximation. This amounts to replacing $\cos(\mathbf{q}\cdot\boldsymbol{\delta})$ in Eqs. (15)–(17) by its expansion truncated just at second order in δ by setting

$$\cos(\mathbf{q}\cdot\boldsymbol{\delta}) \simeq 1 - \tfrac{1}{2}(\mathbf{q}\cdot\boldsymbol{\delta})^2, \quad c(\mathbf{q}) \simeq 1 - \tfrac{1}{2}\langle(\mathbf{q}\cdot\boldsymbol{\delta})^2\rangle. \tag{26}$$

When Eq. (26) is substituted into Eq. (17) for the Helmholtz free energy, the contributions containing $\langle(\mathbf{q}\cdot\boldsymbol{\delta})^2\rangle$ and $\langle(\mathbf{k}\cdot\boldsymbol{\delta})^2\rangle$ cancel out, and we find

$$\frac{\beta F}{N} = \frac{\beta}{v}\sum_{\mathbf{k}} \widetilde{w}(k) - \frac{1}{2}\ln Q - \beta w(0) - \frac{\beta}{2}\delta^2\,\nabla^2 w(r)|_{r=0} + \frac{\beta}{2} w(2\delta), \tag{27}$$

where the term containing ∇^2 originates from recasting in real space the expression $\beta\int \frac{d\mathbf{q}}{(2\pi)^2}(\mathbf{q}\cdot\boldsymbol{\delta})^2\widetilde{w}(q)$, which is obtained by the expansion of the argument of the exponential in Eq. (16). We remark that for the GEM4 interaction this term actually vanishes.

The one-dimer partition function Q is now given by

$$Q = \int_0^{2\pi} d\vartheta \exp\left[\frac{2\beta}{v}\sum_{\mathbf{k}} (\mathbf{k}\cdot\boldsymbol{\delta})^2\widetilde{w}(k)\right], \tag{28}$$

and the probability distribution of dimer orientation is

$$p(\vartheta) = \frac{1}{Q}\exp\left[\frac{2\beta}{v}\sum_{\mathbf{k}} (\mathbf{k}\cdot\boldsymbol{\delta})^2\widetilde{w}(k)\right]. \tag{29}$$

A feature that considerably simplifies the present theory with respect to the more general treatment of Eqs. (15)–(18), is that there is no self-consistency condition akin to Eq. (18) to be enforced. Such a condition would stem from the term containing $\langle(\mathbf{k}\cdot\boldsymbol{\delta})^2\rangle(\mathbf{k}\cdot\boldsymbol{\delta})^2$ in the argument of the exponential of Eq. (29), which here is disregarded since it is of order higher than δ^2. One may say equivalently that at order δ^2 the self-consistency condition becomes trivial, because it reduces to the definition of $\langle(\mathbf{k}\cdot\boldsymbol{\delta})^2\rangle$ in terms of $p(\vartheta)$. Clearly, Eq. (27) still needs to be optimized with respect to the crystal lattice.

Let us now focus on the integral of Eq. (28). Its argument contains the sum

$$\sum_{\mathbf{k}} (\mathbf{k}\cdot\boldsymbol{\delta})^2\widetilde{w}(k) = \sum_{\alpha,\gamma=1}^{2}\sum_{\mathbf{k}} \widetilde{w}(k) k_\alpha k_\gamma \delta_\alpha\delta_\gamma = \boldsymbol{\delta}^{\mathrm{T}}\cdot\mathbf{C}\cdot\boldsymbol{\delta}, \tag{30}$$

where the indexes α, γ denote the components of the vectors $\mathbf{k}$, $\boldsymbol{\delta}$, and $\mathbf{C}$ is the 2×2 matrix with elements $c_{\alpha\gamma}$ given by

$$c_{\alpha\gamma} = \sum_{\mathbf{k}} \widetilde{w}(k) k_\alpha k_\gamma. \tag{31}$$

Since $\mathbf{C}$ is symmetric, it is diagonalized by a rotation. Let Λ_1 and Λ_2 be the (real) eigenvalues of $\mathbf{C}$ corresponding respectively to the 11 and 22 position on the diagonal. We then have

$$\boldsymbol{\delta}^{\mathrm{T}}\cdot\mathbf{C}\cdot\boldsymbol{\delta} = \frac{\delta^2}{2}\{\,\Lambda_1 + \Lambda_2 - (\Lambda_2 - \Lambda_1)\cos\left[2(\vartheta - \varphi)\right]\,\}, \tag{32}$$

where φ is the angle between the eigenvector corresponding to Λ_1 and the x axis. By inserting Eq. (32) into Eq. (28) we obtain

$$Q = 2\pi \exp\left[\frac{\beta}{v}\delta^2 \sum_{\mathbf{k}} k^2 \widetilde{w}(k)\right] I_0\left(\frac{\beta}{v}\delta^2 \Lambda\right), \tag{33}$$

where $I_0(x)$ is the modified Bessel function of order 0,

$$I_0(x) \equiv J_0(ix) = \frac{1}{2\pi}\int_0^{2\pi} d\vartheta\, e^{x\cos\vartheta}, \tag{34}$$

and we have set $\Lambda \equiv \Lambda_2 - \Lambda_1$. If Eq. (33) is substituted into Eq. (27), then we obtain for the Helmholtz free energy

$$\frac{\beta F}{N} = \frac{\beta}{v}\sum_{\mathbf{k}} \widetilde{w}(k)\left[1 - \frac{1}{2}(k\delta)^2\right] - \frac{1}{2}\ln\left[I_0\left(\frac{\beta}{v}\delta^2\Lambda\right)\right] - \beta w(0) - \frac{\beta}{2}\delta^2 \nabla^2 w(r)|_{r=0} + \frac{\beta}{2} w(2\delta) - \frac{1}{2}\ln(2\pi), \tag{35}$$

or, by virtue of Poisson identity,

$$\frac{\beta F}{N} = \beta \sum_{\mathbf{R}\neq\mathbf{0}} w(R) + \frac{\beta}{2}\delta^2 \sum_{\mathbf{R}\neq\mathbf{0}} \nabla^2 w(R) - \frac{1}{2}\ln\left[I_0\left(\frac{\beta}{v}\delta^2\Lambda\right)\right] + \frac{\beta}{2} w(2\delta) - \frac{1}{2}\ln(2\pi). \tag{36}$$

In the numerical evaluation of F, Eq. (36) has been preferred to Eq. (35) not only because the lattice sums are more rapidly convergent in real space but, more importantly, also because Eq. (36) does not require the numerical evaluation of $\widetilde{w}(k)$. In general, this would not be an issue, but is relevant in the present situation, in which, for small δ, F must be mapped with extremely high accuracy to establish if the phase transition takes place.

By inserting Eqs. (32) and (33) into Eq. (29), the probability distribution $p(\vartheta)$ becomes

$$p(\vartheta) = \frac{\exp\left\{-\frac{\beta}{v}\delta^2\Lambda\cos\left[2(\vartheta-\varphi)\right]\right\}}{2\pi I_0\left(\frac{\beta}{v}\delta^2\Lambda\right)}. \tag{37}$$

From Eqs. (35) and (36), Λ emerges as the natural order parameter of the structural transition. Consider the triangular lattice: in this case, because of Eq. (24), the matrix $\mathbf{C}$ is a multiple of the identity, Λ vanishes, and so does the logarithmic term $\ln[\, I_0(\beta\delta^2\Lambda/v)\,]$ in the Helmholtz free energy F. Since $I_0(x) > 1$ for $x \neq 0$, that term always favors nontriangular lattices such that $\Lambda \neq 0$. This, however, is contrasted by the lattice sum in the expression of F, for which the triangular lattice is always the optimal choice. Which effect prevails will be determined by temperature.

Moreover, Eq. (37) for $p(\vartheta)$ shows that the occurrence of this structural transition coincides with that of nematic orientational order. For the triangular lattice such that $\Lambda = 0$, Eq. (37) gives a uniform $p(\vartheta)$, which obviously corresponds to an orientationally disordered phase. As discussed in Sec. III A, strictly speaking $p(\vartheta)$ is never uniform, not even for the triangular lattice, but to make this evident one should consider a description accurate at least to order δ^6, which is well beyond the quadrupole approximation considered here. Nevertheless, the exact $p(\vartheta)$ would still give no macroscopic orientational order, consistently with what is found here.

For $\Lambda \neq 0$, $p(\vartheta)$ instead develops a peak along a certain direction. For $\Lambda < 0$, the distribution is peaked at $\vartheta = \varphi$, $\vartheta = \varphi + \pi$, i.e., the direction is that of the eigenvector corresponding to Λ_1. For $\Lambda > 0$, the distribution is peaked at $\vartheta = \varphi + \pi/2$, $\vartheta = \varphi + 3\pi/2$, i.e., the direction is that of the eigenvector corresponding to Λ_2. In other words, the direction of nematic order is always that of the eigenvector of $\mathbf{C}$ corresponding to its larger eigenvalue.

The link between the structural transition and the nematic order is further stressed by introducing the nematic order parameter $\mathbf{Q}$. In 2D, $\mathbf{Q}$ is a 2×2 matrix whose elements $\mathsf{q}_{\alpha\gamma}$ are given by

$$\mathsf{q}_{\alpha\gamma} = \begin{cases} 2\langle n_\alpha n_\gamma\rangle - 1 & \alpha = \gamma, \\ 2\langle n_\alpha n_\gamma\rangle & \alpha \neq \gamma, \end{cases} \tag{38}$$

where $\mathbf{n} = \boldsymbol{\delta}/\delta$ is a unit vector with the same direction as $\boldsymbol{\delta}$. We have then

$$\begin{aligned} \mathsf{q}_{11} &= \langle\cos(2\vartheta)\rangle, \\ \mathsf{q}_{22} &= -\mathsf{q}_{11} = -\langle\cos(2\vartheta)\rangle, \\ \mathsf{q}_{12} &= \mathsf{q}_{21} = \langle\sin(2\vartheta)\rangle. \end{aligned} \tag{39}$$

The nematic order parameter is defined so that in the disordered phase all its elements vanish, whereas in the nematic phase its larger eigenvalue and the corresponding eigenvector give respectively the amount and the direction of the orientational order. In light of the discussion above, the eigenvectors of $\mathbf{Q}$ must then be same as those of $\mathbf{C}$. Indeed, from Eq. (37) one finds immediately that $\mathbf{Q}$ is diagonalized by setting $\varphi = 0$, i.e., by taking the axes along the eigenvectors of $\mathbf{C}$. The larger eigenvalue of $\mathbf{Q}$, generally referred to as the scalar order parameter S, coincides with q_{22} for $\Lambda > 0$ and with q_{11} for $\Lambda < 0$, and is given by

$$S = \pm\frac{I_0'\left(\frac{\beta}{v}\delta^2\Lambda\right)}{I_0\left(\frac{\beta}{v}\delta^2\Lambda\right)}, \tag{40}$$

where the prime denotes the derivative of $I_0(x)$, and $+$ and $-$ signs refer respectively to $\Lambda > 0$ and $\Lambda < 0$. Hence, S is a function of Λ such that $S \neq 0$ if and only if $\Lambda \neq 0$.

To determine Λ, the Helmholtz free energy given by Eqs. (35) and (36) must be optimized with respect to the crystal structure. As discussed in Sec. III A, in general this requires minimizing F with respect to the quantities a and s which determine the matrices $\mathbf{A}$, $\mathbf{B}$ of the primitive vectors of the direct and reciprocal lattices according to Eq. (19). Let $\mathbf{u}_1$ and $\mathbf{u}_2$ be the primitive vectors of the direct lattice. If the lattice is triangular, the vectors $\mathbf{u}_1$, $\mathbf{u}_2$, and $\mathbf{u}_2 - \mathbf{u}_1$ form an equilateral triangle with a side lying along the x axis. As a and s are changed, that triangle undergoes all the possible deformations that keep its area constant.

In the following, inspired by the results at $T = 0$ summarized in Sec. I, we shall select from the outset the centered rectangular lattice as the only competitor of the triangular lattice. Hence, we shall consider only the deformations such that the equilateral triangle becomes isosceles, and shall take the x axis along the direction of the odd side. For this class of deformations, s remains fixed at the value $s = 1/2$ of the

triangular lattice, and the only free parameter is the lattice constant a. Compared to the equilateral case, the triangle splays for $a > a_0$, and tapers for $a < a_0$. For both the direct and the reciprocal lattices, the conventional unit cell is a rectangle with sites at the vertexes and at the center, whose sides lie along the x- and y-axes. Clearly, if (k_x, k_y) is a point of the reciprocal lattice, then the same holds for the points $(-k_x, k_y)$ and $(k_x, -k_y)$. Because of Eq. (31), we have then $c_{12} = c_{21} = 0$, $c_{11} = \Lambda_1$, $c_{22} = \Lambda_2$, so that the matrix $\mathbf{C}$ is diagonal from the outset, and its eigenvectors are directed along the sides of the conventional cell, i.e., along the odd side of the triangle and along its height. Moreover, the structural order parameter Λ coincides with the quantity λ given by

$$\lambda = c_{22} - c_{11} = \sum_{\mathbf{k}} \left(k_y^2 - k_x^2\right) \widetilde{w}(k), \tag{41}$$

or, using again Poisson identity,

$$\lambda = v \sum_{\mathbf{R}} \left(\frac{\partial^2}{\partial x^2} - \frac{\partial^2}{\partial y^2} \right) w(R). \tag{42}$$

In the following, unless otherwise stated, we shall use λ as defined in Eqs. (41) and (42) to refer to the order parameter Λ.

C. Landau expansion

Within the quadrupole approximation introduced in Sec. III B, the numerical minimization of the Helmholtz free energy F and the determination of the structural and nematic order parameters λ and S can be carried out rather straightforwardly. Before doing so, further insight into the nature of the transition can be gained by performing a Landau expansion of F in powers of λ.

If we consider Eq. (35) for F, the terms in the second line do not depend on λ, since they are lattice-independent. The logarithmic term is expanded in powers of its argument via the McLaurin expansion of $I_0(x) = 1 + x^2/4 + x^4/64 + \cdots$:

$$-\frac{1}{2} \ln \left[I_0\left(\frac{\beta}{v} \delta^2 \lambda \right) \right] = -\frac{1}{8} \left(\frac{\beta}{v} \delta^2 \lambda \right)^2 + \frac{1}{128} \left(\frac{\beta}{v} \delta^2 \lambda \right)^4 + \cdots, \tag{43}$$

and contains only even powers of λ, so that its first derivative with respect to λ vanishes at $\lambda = 0$.

The expansion of the lattice sums in Eq. (35) is more involved. Let us set

$$\mathcal{F} = \sum_{\mathbf{k}} f(k), \quad f(k) = \widetilde{w}(k) \left[1 - \frac{1}{2} (k\delta)^2 \right]. \tag{44}$$

Using Eq. (19), we obtain for the derivative of the wave vector $\mathbf{k}$ with respect to the lattice constant a,

$$\frac{d}{da} \begin{pmatrix} k_x \\ k_y \end{pmatrix} = \frac{d\mathbf{B}}{da} \mathbf{B}^{-1} \begin{pmatrix} k_x \\ k_y \end{pmatrix} = \frac{1}{a} \begin{pmatrix} -k_x \\ k_y \end{pmatrix}. \tag{45}$$

Differentiating with respect to a Eqs. (41) and (44) gives

$$\frac{d\mathcal{F}}{da} = \frac{2}{a} S_1 \left[\frac{d f}{d(k^2)} \right], \quad \frac{d\lambda}{da} = \frac{2}{a} S_2[\widetilde{w}], \tag{46}$$

where we have introduced the functionals

$$S_1[g] = \sum_{\mathbf{k}} \left(k_y^2 - k_x^2\right) g(k), \tag{47}$$

$$S_2[g] = \frac{a}{2} \frac{d}{da} S_1[g] = \sum_{\mathbf{k}} \left[\left(k_y^2 - k_x^2\right)^2 \frac{dg(k)}{d(k^2)} + k^2 g(k) \right], \tag{48}$$

$g(k)$ being a generic spherically symmetric function such that the sums over $\mathbf{k}$ are convergent. For the triangular lattice, it is found that $S_2[\widetilde{w}] \neq 0$. Hence, in the neighborhood of the triangular lattice the mapping $a \to \lambda$ is invertible, and one has

$$\frac{d\mathcal{F}}{d\lambda} = S_1 \left[\frac{d f}{d(k^2)} \right] \frac{1}{S_2[\widetilde{w}]}. \tag{49}$$

Moreover, Eqs. (24) and (47) imply that on the triangular lattice $d\mathcal{F}/da = d\mathcal{F}/d\lambda = 0$. Putting together the lattice-sum and the logarithmic contributions to F, we find

$$\left. \frac{dF}{d\lambda} \right|_{\lambda=0} = 0, \tag{50}$$

so that the triangular lattice always represents a stationary point of the Helmholtz free energy F, as one would expect. Whether such a points corresponds to the absolute minimum depends on the higher-order derivatives of F with respect to λ. The expressions of the second, third, and fourth derivatives of the lattice-sum term $\mathcal{F}$ are provided in Appendix A.

Aside of their rather involved form, what actually matters here is the sign of those derivatives. Using Eqs. (A6)–(A8) we find

$$\left. \frac{d^2\mathcal{F}}{d\lambda^2} \right|_{\lambda=0} > 0, \quad \left. \frac{d^3\mathcal{F}}{d\lambda^3} \right|_{\lambda=0} < 0, \quad \left. \frac{d^4\mathcal{F}}{d\lambda^4} \right|_{\lambda=0} > 0. \tag{51}$$

We notice that, unlike the logarithm $\ln[I_0(\beta\delta^2\lambda/v)]$, the lattice sum $\mathcal{F}$ contains a cubic term in λ. By taking into account both contributions, we finally obtain the Landau expression of F:

$$\frac{\Delta F}{N} = A\lambda^2 - B\lambda^3 + C\lambda^4, \tag{52}$$

where ΔF is the difference between the actual Helmholtz free energy and the Helmholtz free energy of the triangular lattice, and we have set

$$A = \frac{1}{2v} \left(\left. \frac{d^2\mathcal{F}}{d\lambda^2} \right|_{\lambda=0} - \frac{1}{4} \frac{\beta}{v} \delta^4 \right), \tag{53}$$

$$B = -\frac{1}{6v} \left. \frac{d^3\mathcal{F}}{d\lambda^3} \right|_{\lambda=0}, \tag{54}$$

$$C = \frac{1}{8v} \left[\frac{1}{3} \left. \frac{d^4\mathcal{F}}{d\lambda^4} \right|_{\lambda=0} + \frac{1}{16} \left(\frac{\beta}{v} \right)^3 \delta^8 \right]. \tag{55}$$

Equations (51) and (53) imply that, as the temperature T decreases, A turns from positive to negative, and vanishes at a temperature T' given by

$$k_B T' = \frac{\delta^4}{4v} \left(\frac{d^2\mathcal{F}}{d\lambda^2} \right)^{-1}_{\lambda=0}, \tag{56}$$

whereas B and C are both positive at every T. Hence, ΔF has the standard form which describes a first-order phase transition: at high T, ΔF displays only one minimum at $\lambda = 0$ but,

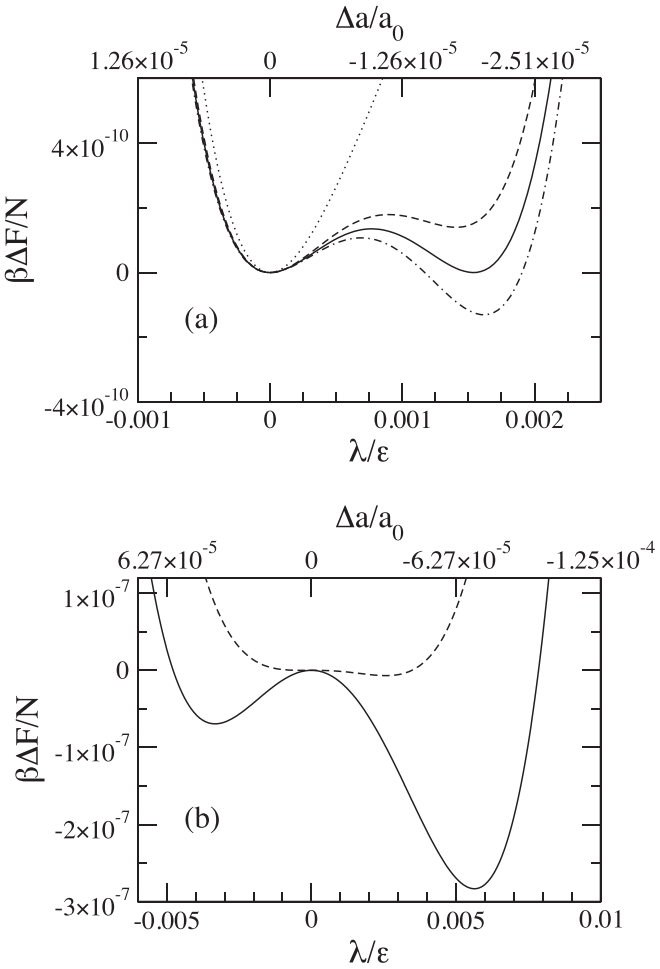

FIG. 1. Difference $\beta\Delta F/N$ between the Helmholtz free energy per particle and unit temperature of the dimer crystal at fixed density $\rho = 1.13971R^{-2}$ and dimer length $2\delta = 0.05R$ on a centered rectangular lattice, and the same quantity on the triangular lattice. $\beta\Delta F/N$ given by Eqs. (35) and (36) has been displayed as a function of the structural order parameter λ defined in Eqs. (41) and (42). The upper axis reports the relative difference $\Delta a/a_0$ of the lattice constant a with respect to the value $a_0 = 1.4234837R$ pertaining to the triangular lattice. The various curves refer to different temperatures. (a) Dotted curve, $k_BT/\varepsilon = 2.38938 \times 10^{-5}$; dashed curve, $k_BT/\varepsilon = 2.38933 \times 10^{-5}$; solid curve, $k_BT/\varepsilon = 2.3893245 \times 10^{-5}$; dash-dotted curve, $k_BT/\varepsilon = 2.38932 \times 10^{-5}$. (b) Dashed curve, $k_BT/\varepsilon = 2.3892 \times 10^{-5}$; solid curve, $k_BT/\varepsilon = 2.388 \times 10^{-5}$.

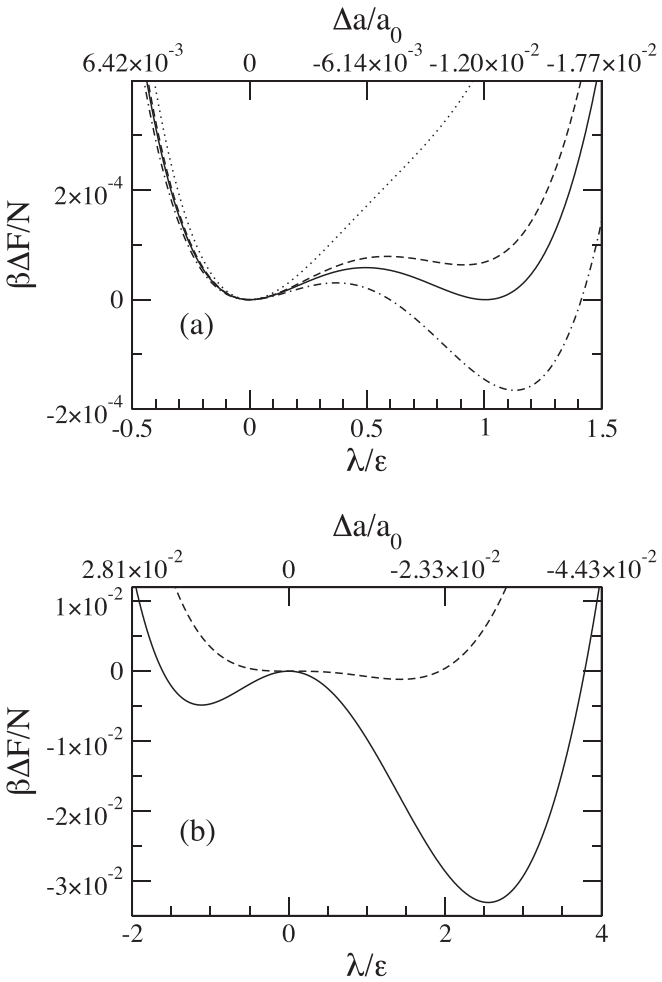

FIG. 2. Same as Fig. 1, but for dimer length $2\delta = 0.25R$ and a different set of temperatures. (a) Dotted curve, $k_BT/\varepsilon = 1.6 \times 10^{-2}$; dashed curve, $k_BT/\varepsilon = 1.584 \times 10^{-2}$; solid curve, $k_BT/\varepsilon = 1.5811 \times 10^{-2}$; dash-dotted curve, $k_BT/\varepsilon = 1.575 \times 10^{-2}$. (b) Dashed curve, $k_BT/\varepsilon = 1.55 \times 10^{-2}$; solid curve, $k_BT/\varepsilon = 1.13 \times 10^{-2}$.

as T is decreased, another minimum at $\lambda \neq 0$ develops due to the λ^3 term. Below a certain temperature T_0, this becomes the absolute minimum, and λ jumps discontinuously from $\lambda = 0$ to the value $\lambda = 2A/B$. At the transition temperature T_0, one has $A = B^2/(4C)$, so that A is still positive, implying that T_0 is higher than the temperature T', at which the minimum at $\lambda = 0$ becomes unstable.

This qualitative picture based on the Landau expansion (52) is confirmed by the behavior of ΔF obtained from Eq. (36), which we have displayed in Figs. 1 and 2 as a function of the order parameter λ for different temperatures and dimer length $2\delta = 0.05R$ and $2\delta = 0.25R$, R being the range of the GEM4 potential. Above the upper axis we have also reported the values of the relative difference $\Delta a/a_0$ of the lattice constant a with respect to the value a_0 pertaining to the triangular lattice. Since for this lattice $S_2[\widetilde{w}]$ is negative, Eq. (46) implies that $d\lambda/da$ is also negative, i.e., a positive value of λ corresponds to $a < a_0$, and a negative value to $a > a_0$.

For both values of δ, the scenario is undoubtedly that of a first-order phase transition, albeit a rather weak one on purely quantitative terms. In particular, in the short-dimer case $2\delta = 0.05R$ already considered in Ref. [18], the first-order character is *extremely weak:* the transition temperature $k_BT_0/\varepsilon = 2.3893245 \times 10^{-5}$ is hardly distinguishable from the stability threshold of the triangular lattice $k_BT'/\varepsilon = 2.3892460 \times 10^{-5}$. At the transition, the free-energy barrier between the two minima is just slightly above a mere $\beta\Delta F/N \sim 10^{-10}$, and the order parameter λ jumps from $\lambda = 0$ to $\lambda/\varepsilon \sim 1.5 \times 10^{-3}$, corresponding to a relative change in the lattice constant $\Delta a/a_0 \sim -2 \times 10^{-5}$. In such a situation, we expect that telling between a first- and a second-order phase transition

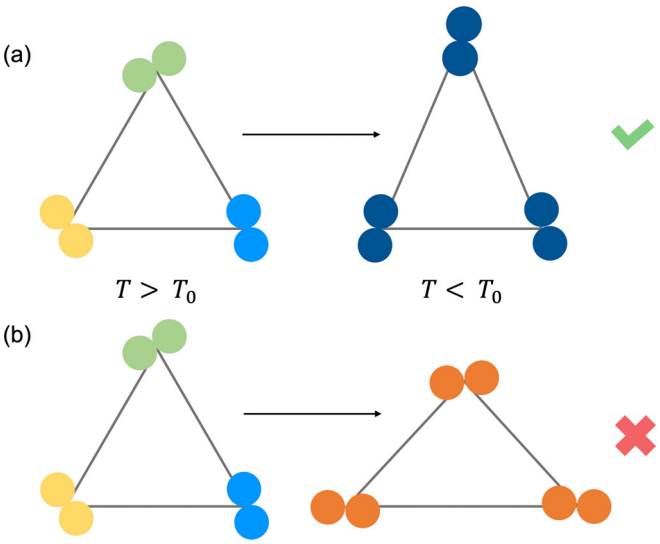

FIG. 3. (a) Schematic depiction of the structural and orientational transition. Above the transition temperature T_0, the dimers are arranged on a triangular lattice and have no orientational order. Below T_0, the equilateral triangles of the triangular lattice become isosceles by making the horizontal side shorter than the other two, and the dimers align along the vertical direction. (b) Depiction of the hypothetical transition corresponding to the metastable minimum of the free energy, which instead is not realized. The horizontal side of the equilateral triangles becomes longer than the other two, and the dimers align along the horizontal direction.

would prove exceedingly difficult not only in an experiment, but also in a simulation.

Not surprisingly, the situation becomes less extreme for longer dimers: for $2\delta = 0.25R$, we find $k_B T_0/\varepsilon = 1.5811 \times 10^{-2}$, $k_B T'/\varepsilon = 1.5431 \times 10^{-2}$, $\beta\Delta F/N \sim 6 \times 10^{-5}$ for the free-energy barrier between the two minima at the transition, and a jump in the order parameter $\lambda/\varepsilon \sim 1$, corresponding to $\Delta a/a_0 \sim -1.2 \times 10^{-2}$. Still, the dimer length cannot be increased at one's will, since in the theory it is assumed from the outset that contact between dimers lying on neighboring sites does not occur.

As discussed above, the negative value of Δa is due to the positive value of λ at the transition. Hence, at the transition the equilateral triangles of the triangular lattice turn into isosceles in such a way, that the odd side becomes shorter than the other two, i.e., the triangles taper. Moreover, according to the discussion carried out in Sec. III B, a positive λ implies that the direction of nematic order is that of the eigenvector corresponding to λ_2. For the case in hand in which the matrix $\mathbf{C}$ is diagonal from the outset, this is just the direction of the y axis, namely, that orthogonal to the odd side. The transition is depicted schematically in Fig. 3(a).

Below T', the triangular lattice such that $\lambda = 0$ is not a minimum of F any more, and another minimum develops, this time with $\lambda < 0$. Hence, below T' both minima are located at $\lambda \neq 0$, either positive or negative, as illustrated in Figs. 1(b) and 2(b). Following again the discussion in Sec. III B, the minimum with $\lambda < 0$ corresponds to a lattice with $\Delta a > 0$, and the nematic director along the x axis. In other words, a transition to this minimum would have the triangles splay instead of tapering, and the dimers align along the direction of the odd side, rather than along the direction orthogonal to it, as displayed in Fig. 3(b). Such a transition does not occur, because the free energy of this local minimum is always larger than that of the minimum with $\lambda > 0$. Actually, as will be discussed in Sec. III D, the local minimum is even revealed to be unstable as soon as the $s = 1/2$ constraint in Eq. (19) is released, and one moves to the space of all possible lattice deformations. The present scenario is consistent with that observed at $T = 0$ [18], whereby the system was always found to choose the configuration described by the minimum with $\lambda > 0$, unlike what one would expect in a second-order transition.

A natural question that can be addressed straightforwardly by the Landau approach, is how the transition temperature T_0 and the order parameter at the transition $\lambda(T_0^-)$ depend on δ. In general, determining T_0 from Eq. (52) with A, B, C given by Eqs. (53)–(55) requires solving a fourth-order degree equation, but the results for T_0 given above show that, even for relatively long dimers such that $2\delta = 0.25R$, T_0 remains close to the temperature T' given by Eq. (56), so that the correction to T' can be regarded as a perturbation. Hence, to leading order in δ one has $T_0 \simeq T' \sim \delta^4$. However, to obtain the corresponding scaling of λ this correction must be taken into account, since at the transition one has $\lambda = 2A/B$, and A vanishes at T'. By including in T_0 the next-to-leading order term, we find

$$T_0 \simeq T'\left[1 + \frac{\delta^4}{36}\left(\frac{d^3\mathcal{F}}{d\lambda^3}\right)^2_{\lambda=0}\left(\frac{d^2\mathcal{F}}{d\lambda^2}\right)^{-4}_{\lambda=0}\right] \sim \mathcal{O}(\delta^4), \quad (57)$$

$$\lambda(T_0^-) \simeq -\frac{\delta^4}{6}\left(\frac{d^3\mathcal{F}}{d\lambda^3}\right)_{\lambda=0}\left(\frac{d^2\mathcal{F}}{d\lambda^2}\right)^{-3}_{\lambda=0} \sim \mathcal{O}(\delta^4), \quad (58)$$

showing that, to leading order in δ, both T_0 and $\lambda(T_0^-)$ are proportional to δ^4.

The behavior of the specific heat per particle at constant volume c_V is also worth considering. Here and in the following, the trivial contribution to the specific heat due to the kinetic energy will be disregarded, and we shall focus solely on its configurational part. From Eqs. (52)–(55) we obtain for the Landau expression of c_V

$$c_V = k_B\,\lambda\frac{\theta^2}{\delta^4}\left(1 - \frac{3}{2}\lambda^2\frac{\theta^2}{\delta^4}\right) \times \frac{\theta + \lambda\left[\frac{d^3\mathcal{F}}{d\lambda^3}\big|_{\lambda=0} + 2\lambda\left(\frac{1}{3}\frac{d^4\mathcal{F}}{d\lambda^4}\big|_{\lambda=0} - \frac{\theta^3}{4\delta^4}\right)\right]}{\frac{d^3\mathcal{F}}{d\lambda^3}\big|_{\lambda=0} + 2\lambda\left(\frac{1}{3}\frac{d^4\mathcal{F}}{d\lambda^4}\big|_{\lambda=0} + \frac{\theta^3}{2\delta^4}\right)}, \quad (59)$$

where we have set $\theta = \beta\delta^4/(2v)$. At the transition, c_V has a discontinuity. For $T > T_0$, λ vanishes identically, so that c_V also vanishes. For $T \to T_0^-$, substitution of Eqs. (57) and (58) into Eq. (59) gives

$$c_V(T_0^-) = 4k_B + \mathcal{O}(\delta^4). \quad (60)$$

Therefore, the discontinuity in c_V survives even for $\delta \to 0$, attaining the interaction-independent value $4k_B$. This may at first appear surprising, but it does not contradict the fact that for $\delta = 0$ there is no transition at all, since T_0 vanishes for $\delta \to 0$. Moreover, such a behavior is consistent with the fact that, as discussed above, as δ decreases the first-order transi-

tion becomes more and more similar to a second-order one, for which Landau theory does predict a finite discontinuity for c_V.

To avoid redundancy, the behavior of the structural order parameter λ, the nematic order parameter S, and the specific heat c_V as a function of temperature will be displayed in Sec. V, after the effect of lattice and dimer vibrations has been taken into account in Sec. III E.

D. Stability of the free-energy minimum

The first-order transition described in Sec. III C clearly resembles the isotropic-nematic transition in liquid crystals, which is also first order. However, the two systems differ in an important respect: in liquid crystals, the nematic director is equally likely to point in any direction, i.e., the transition entails the breaking of a continuous symmetry. Here, by contrast, the director can point only along the direction orthogonal to the shorter side of the triangle, so that there are just three possible directions, depending on which side of the triangle becomes shorter than the other two at the transition, as illustrated in Fig. 5 of Ref. [18]. Therefore, the transition must occur via the breaking of a discrete symmetry, specifically a threefold one, similarly to the Potts model. This situation bears a strong resemblance with the occurrence of nematic states in the two-dimensional antiferromagnet $Fe_{1/3}NbS_2$, which was observed experimentally and discussed theoretically in Ref. [22].

Alas, this threefold-symmetry-breaking process is not accounted for by the Landau free energy obtained in Sec. III C, because for the sake of simplicity the identity of the shorter side of the triangle, and hence the direction of nematic order, were picked out beforehand, as discussed at the end of Sec. III B. To incorporate it, one should consider all possible lattice deformations that keep the area of the primitive cell constant, thereby releasing the $s = 1/2$ constraint in Eq. (19) and adding one degree of freedom to the free energy. As a consequence, the direction of the eigenvector corresponding to the larger eigenvalue of the matrix $\mathbf{C}$, which identifies the nematic director, should be determined *a posteriori*. Obtaining the expression of the Landau free energy then becomes a much more involved problem, and we have postponed it to a subsequent investigation.

Nevertheless, we acknowledge that it could be questioned whether the scenario described in Sec. III C would still hold, once this extra degree of freedom is taken into account. Since the nematic state was obtained as a minimum of the free energy in a one-dimensional space, how can one be sure that such a state would remain a minimum also in the two-dimensional space of all possible lattices? Dismissing this question would clearly be inappropriate, even assuming that one does not undertake the task of obtaining the general form of the Landau free energy.

To tackle this point, we studied the stability of the minima at $\lambda \neq 0$ discussed in Sec. III C in the two-parameter space spanned by a and s. In the more general situation where s is not locked at $s = 1/2$, the directions of the eigenvectors of $\mathbf{C}$ do not necessarily coincide with those of the coordinate axes. Similarly, the order parameter Λ, i.e., the difference between the eigenvalues of $\mathbf{C}$, does not generally coincide with λ as defined in Eqs. (41) and (42), but is given by $\Lambda = \pm\sqrt{\lambda^2 + \mu^2}$, with μ defined by

$$\mu = 2\sum_{\mathbf{k}} k_x k_y \widetilde{w}(k) = -2v \sum_{\mathbf{R}} \frac{\partial^2}{\partial x \partial y} w(R). \tag{61}$$

Following the lines laid out in Sec. III C, we switch from the variables (a, s) to the variables (λ, μ). Let us denote by λ_+ the minimum at $\lambda > 0$ which becomes the absolute minimum below the transition temperature T_0, and by λ_- the local minimum at $\lambda < 0$ which develops below the temperature T', at which the triangular lattice at $\lambda = 0$ becomes unstable. Since these minima were obtained in the subspace $\mu = 0$, one has

$$\left.\frac{\partial F}{\partial \lambda}\right|_{\lambda,0} = \frac{dF}{d\lambda}(\lambda, \mu = 0) = 0, \tag{62}$$

$$\left.\frac{\partial^2 F}{\partial \lambda^2}\right|_{\lambda,0} = \frac{d^2F}{d\lambda^2}(\lambda, \mu = 0) > 0, \tag{63}$$

for both $\lambda = \lambda_+$ and $\lambda = \lambda_-$. Whether such states will correspond to minima of F also in the two-dimensional space of all possible lattices hinges on the derivatives of F with respect to μ. The expressions of those derivatives have been provided in Appendix B. By evaluating them at $\lambda = \lambda_+, \mu = 0$ and $\lambda = \lambda_-, \mu = 0$, the following results are obtained: as far as the first derivatives are concerned, we find

$$\left.\frac{\partial F}{\partial \mu}\right|_{\lambda_+,0} = \left.\frac{\partial F}{\partial \mu}\right|_{\lambda_-,0} = 0, \tag{64}$$

so that the states in hand are indeed stationary points of F. For the second derivatives, we find

$$\left.\frac{\partial^2 F}{\partial \lambda \partial \mu}\right|_{\lambda_+,0} = \left.\frac{\partial^2 F}{\partial \lambda \partial \mu}\right|_{\lambda_-,0} = 0, \tag{65}$$

$$\left.\frac{\partial^2 F}{\partial \mu^2}\right|_{\lambda_+,0} > 0, \quad \left.\frac{\partial^2 F}{\partial \mu^2}\right|_{\lambda_-,0} < 0. \tag{66}$$

Equations (65) and (66) show that the state at $\lambda = \lambda_+$, $\mu = 0$ which, below T_0, gives the absolute minimum of F in the subspace $\mu = 0$, remains a minimum even in the two-dimensional (λ, μ) space. Interestingly, they also show that this does not apply to the state at $\lambda = \lambda_-$, $\mu = 0$, which instead is revealed to be a saddle point as soon as one moves away from the $\mu = 0$ subspace.

Besides the study described above, we checked the stability of the minimum obtained in Sec. III C also by minimizing numerically Eq. (36) for F in the (a, s) space of all possible two-dimensional lattices compatible with the constant-area requirement. Above the transition temperature T_0, we found that the minimum of F is given by the triangular lattice with $a = a_0$ and no orientational order. Below T_0, we did find that the absolute minimum is reached at three degenerate states with nematic order: one of them is located at $s = 1/2$ and $a = \overline{a}$ such that $\lambda = \lambda_+$, and coincides with the one considered here. The other two correspond respectively to $s = s'$, $a = a'$ and $s = 1 - s'$, $a = a'$, where a' and s' are given by

$$a' = \frac{\overline{a}}{2}\left[1 + 3\left(\frac{a_0}{\overline{a}}\right)^4\right]^{1/2}, \quad s' = \left[1 - \frac{3}{4}\left(\frac{a_0}{a'}\right)^4\right]^{1/2} \tag{67}$$

and are obtained by deforming the equilateral triangle of the triangular lattice along either of its sides which are not aligned

with the x axis. This analysis leads us to conclude that the centered rectangular lattice considered here is the *bona fide* minimum of F at sufficiently low temperature.

E. Inclusion of lattice and dimer vibrations

In Secs. III A–III D we have focused only on the orientational degrees of freedom of the dimers. However, the main feature of $Q^{\pm}$ potentials such as the GEM4 interaction considered here is that cluster crystals are formed spontaneously at low temperature. Hence, to make contact with the actual system, we should not regard the position or the length of the dimers as given *a priori*, but should instead take into account that both of them are actually state-dependent quantities, to be determined by thermal averages of the microscopic particle configurations.

Since the temperature T_0 of the nematic transition is much lower than that at which the dimer crystal forms, we can safely assume that, in the temperature regime pertaining to this study, both the position of the dimer center and the separation between the dimer particles consist in small displacements from their equilibrium values at $T = 0$. In the absence of a hard core, a thorough study of lattice and intracluster oscillations in $Q^{\pm}$ potentials was carried out in Ref. [20]. Here, instead, we do not aim at a detailed description of the phonon spectrum, but just at including the main consequences of regarding the dimer position and length as dynamical variables into the present mean-field description.

If neither the position of the dimer center nor its length are fixed, Eq. (4) for the position $\mathbf{x}_{i,\sigma}$ of the dimer particles at site i is replaced by

$$\mathbf{x}_{i,\sigma} = \mathbf{R}_i + \boldsymbol{\xi}_i + \sigma\boldsymbol{\eta}_i, \quad \sigma \pm 1, \tag{68}$$

where $\boldsymbol{\xi}_i$ denotes the displacement of the dimer center from its equilibrium position at $\mathbf{R}_i$, and $\boldsymbol{\eta}_i$ is the vector connecting the dimer center with particle 1. The orientation of $\boldsymbol{\eta}_i$ with respect to the x axis is still specified by the angle ϑ_i, while its length η does not necessarily coincide with the hard-core radius δ. Equation (5) for the potential energy of the system corresponding to a given microscopic configuration then becomes

$$U = \frac{1}{2}\sum_{i\neq j,\sigma,\sigma'} w(\mathbf{R}_i - \mathbf{R}_j + \boldsymbol{\xi}_i - \boldsymbol{\xi}_j + \sigma\boldsymbol{\eta}_i - \sigma'\boldsymbol{\eta}_j) + \frac{N}{2}w(2\eta). \tag{69}$$

We now consider the probability distribution $P(\boldsymbol{\xi}_1, \boldsymbol{\eta}_1 \ldots \boldsymbol{\xi}_{N/2}, \boldsymbol{\eta}_{N/2})$ of the dimer configurations and make again use of Gibbs' variational principle by representing it as the product of $N/2$ independent contributions:

$$P(\boldsymbol{\xi}_1, \boldsymbol{\eta}_1 \ldots \boldsymbol{\xi}_{N/2}, \boldsymbol{\eta}_{N/2}) = \mathsf{p}(\boldsymbol{\xi}_1, \boldsymbol{\eta}_1) \times \cdots \times \mathsf{p}(\boldsymbol{\xi}_{N/2}, \boldsymbol{\eta}_{N/2}). \tag{70}$$

Moreover, also the one-dimer probability distribution $\mathsf{p}(\boldsymbol{\xi}, \boldsymbol{\eta})$ is factorized as the product of three independent distributions via the assumption

$$\mathsf{p}(\boldsymbol{\xi}, \boldsymbol{\eta}) = p_{\mathrm{D}}(\boldsymbol{\xi})\, p_{\mathrm{L}}(\eta)\, p(\vartheta), \tag{71}$$

where $p_{\mathrm{D}}(\boldsymbol{\xi})$ is the probability distribution of the position of the center of the dimer with respect to the lattice site at $\mathbf{R}$, $p_{\mathrm{L}}(\eta)$ is the probability distribution of the dimer length, and $p(\vartheta)$ is the probability distribution of the dimer orientation as before. We then have

$$\langle \ln P\rangle = \frac{N}{2}\left[\int d\boldsymbol{\xi}\, p_{\mathrm{D}}(\boldsymbol{\xi}) \ln p_{\mathrm{D}}(\boldsymbol{\xi}) + \int_{\delta}^{+\infty} d\eta\, \eta\, p_{\mathrm{L}}(\eta) \ln p_{\mathrm{L}}(\eta) + \int_0^{2\pi} d\vartheta\, p(\vartheta) \ln p(\vartheta)\right], \tag{72}$$

where the integral with respect to $\boldsymbol{\xi}$ is extended over the whole plane. For the thermal average $\langle U\rangle$ of the potential energy, we switch again to Fourier space and obtain

$$\langle U\rangle = \frac{N}{v}\sum_{\mathbf{k}} \langle\!\langle \cos(\mathbf{k}\cdot\boldsymbol{\eta})\rangle\!\rangle^2 \widetilde{p}_{\mathrm{D}}^2(\mathbf{k})\widetilde{w}(k) - N\int \frac{d\mathbf{q}}{(2\pi)^2} \langle\!\langle \cos(\mathbf{q}\cdot\boldsymbol{\eta})\rangle\!\rangle^2 \widetilde{p}_{\mathrm{D}}^2(\mathbf{q})\widetilde{w}(q) + \frac{N}{2}\langle w(2\eta)\rangle_{\mathrm{L}}, \tag{73}$$

where $\widetilde{p}_{\mathrm{D}}(\mathbf{q})$ is the Fourier transform of $p_{\mathrm{D}}(\boldsymbol{\xi})$, $\langle\ldots\rangle_{\mathrm{L}}$ denotes the average over η performed by the distribution $p_{\mathrm{L}}(\eta)$, and $\langle\!\langle\ldots\rangle\!\rangle$ denotes the average over $\boldsymbol{\eta}$ performed by the distribution $p_{\mathrm{L}}(\eta)\, p(\vartheta)$.

We now make the following *ansatz* for $p_{\mathrm{D}}(\boldsymbol{\xi})$ and $p_{\mathrm{L}}(\eta)$:

$$p_{\mathrm{D}}(\boldsymbol{\xi}) = \frac{\alpha}{\pi}\, e^{-\alpha\xi^2}, \tag{74}$$

$$p_{\mathrm{L}}(\eta) = \frac{\gamma^2}{1+\gamma\delta}\, e^{-\gamma(\eta-\delta)}, \quad \eta \geqslant \delta, \tag{75}$$

where α and γ are variational parameters to be determined by minimizing the Helmholtz free energy, and the prefactors in front of the exponentials are the normalization constants of the probability distributions. Equation (74) is equivalent to representing the local dimer density as a superposition of Gaussians centered at the lattice sites, which has been shown to be an accurate expression for $Q^{\pm}$ potentials [4,5]. In Ref. [5] it was shown that, at low temperature, this representation is equivalent to Einstein model of crystals, in which the same frequency is assigned to all vibrational modes. As for Eq. (75), the argument of the exponential is linear in $\eta - \delta$, so it does not have a Gaussian form, at variance with Eq. (74). The reason for this choice will be discussed later in Sec. V.

With Eqs. (74) and (75), Eq. (72) becomes

$$\langle \ln P\rangle = N\left[G(\alpha,\nu) + \frac{1}{2}\int_0^{2\pi} d\vartheta\, p(\vartheta)\ln p(\vartheta)\right], \tag{76}$$

where we have set $\nu = \gamma\delta$, and $G(\alpha,\nu)$ is defined as

$$G(\alpha,\nu) = \frac{1}{2}\left[\ln\left(\frac{\alpha}{\pi}\right) + 2\ln\left(\frac{\nu}{\delta}\right) - \ln(1+\nu) - \frac{1}{1+\nu} - 2\right]. \tag{77}$$

Finally, we resort again to the quadrupole approximation (26) by expanding $\cos(\mathbf{k}\cdot\boldsymbol{\eta})$ and $\cos(\mathbf{q}\cdot\boldsymbol{\eta})$ in Eq. (73) to second order in η. For this approximation to make sense, it is required not only that the hard-core radius δ is small

with respect to the interaction range, but also that the average deviation of η from δ is small with respect to δ. This can be verified *a posteriori* as a consistency check of the approximation, see Sec. V. We also note that, for the GEM4 interaction considered here, the first, second, and third derivatives of $w(r)$ at $r = 0$ are all vanishing. Hence, for small η we have

$$\langle w(2\eta)\rangle_{\rm L} = w(0) + \mathcal{O}(\delta^4), \tag{78}$$

where the $\mathcal{O}(\delta^4)$ term can be disregarded at the level of the quadrupole approximation. Therefore, in the following $\langle w(2\eta)\rangle_{\rm L}$ in Eq. (73) will be replaced by $w(0)$.

Because of Eq. (71), the degrees of freedom corresponding to $\boldsymbol{\xi}$, η, and ϑ can be traced out independently of one another, and Eq. (7) gives

$$\begin{aligned}\frac{\beta F}{N} &= \frac{\beta}{v}\sum_{\mathbf{k}} e^{-k^2/(2\alpha)}\,\widetilde{w}(k)[1 - \langle(\mathbf{k}\cdot\boldsymbol{\delta}_{\rm eff})^2\rangle] \\ &\quad - \beta\int \frac{d\mathbf{q}}{(2\pi)^2}\, e^{-q^2/(2\alpha)}\,\widetilde{w}(q)\left[1 - \frac{1}{2}(q\delta_{\rm eff})^2\right] \\ &\quad + G(\alpha,\nu) + \frac{1}{2}\langle \ln p\rangle + \frac{\beta}{2}w(0),\end{aligned} \tag{79}$$

where $\langle\ldots\rangle$ denotes as usual the average over the dimer orientation performed via $p(\vartheta)$, and $\boldsymbol{\delta}_{\rm eff}$ is a vector with the same direction as $\boldsymbol{\delta}$ and modulus given by

$$\delta_{\rm eff} = \left[\int_{\delta}^{+\infty} d\eta\,\eta^3 p_{\rm L}(\eta)\right]^{1/2} = \delta\left[1 + 2\,\frac{\nu^2+3\nu+3}{\nu^2(\nu+1)}\right]^{1/2}. \tag{80}$$

Functional minimization of Eq. (79) with respect to $p(\vartheta)$ leads to

$$\begin{aligned}\frac{\beta F}{N} &= \frac{\beta}{v}\sum_{\mathbf{k}} e^{-k^2/(2\alpha)}\widetilde{w}(k)\left[1 - \frac{1}{2}(k\delta_{\rm eff})^2\right] \\ &\quad - \beta\int \frac{d\mathbf{q}}{(2\pi)^2}\, e^{-q^2/(2\alpha)}\widetilde{w}(q)\left[1 - \frac{1}{2}(q\delta_{\rm eff})^2\right] \\ &\quad - \frac{1}{2}\ln\left[I_0\left(\frac{\beta}{v}\delta_{\rm eff}^2\lambda_{\rm eff}\right)\right] + G(\alpha,\nu) + \frac{\beta}{2}w(0) \\ &\quad - \frac{1}{2}\ln(2\pi).\end{aligned} \tag{81}$$

As discussed at the end of Sec. III B, here we have restricted ourselves to lattice deformations such that the lattice parameter s remains fixed at $s = 1/2$. In that case, the order parameter Λ coincides with λ given by Eq. (41), and $\lambda_{\rm eff}$ is defined as

$$\lambda_{\rm eff} = \sum_{\mathbf{k}} \left(k_y^2 - k_x^2\right) e^{-k^2/(2\alpha)}\widetilde{w}(k). \tag{82}$$

By comparing Eq. (81) with Eq. (35) we see that, aside of the substitution $w(2\delta) \to w(0)$ consistent with the quadrupole approximation and the $G(\alpha,\nu)$ term that accounts for the entropic contribution due to lattice vibrations and fluctuations of the dimer length, the two expressions for $\beta F/N$ are formally identical, provided $\widetilde{w}(k)$ is replaced by $e^{-k^2/(2\alpha)}\widetilde{w}(k)$, and δ is replaced by $\delta_{\rm eff}$. Similarly, the equilibrium probability distribution $p(\vartheta)$ is still given by Eq. (37) with the substitutions $\delta \to \delta_{\rm eff}$ and $\Lambda \to \lambda_{\rm eff}$, and the same applies to the nematic order parameter S given by Eq. (40). Hence, the qualitative features of the structural and nematic transition, including its first-order character, remain the same as those discussed in Sec. III C, as will be shown in Sec. V.

Because of the low temperature of the transition, we expect the width $\sim 1/\sqrt{\alpha}$ of the oscillations of the lattice sites to be much smaller than the lattice constant a. In Eqs. (81) and (82) we can then set

$$e^{-k^2/(2\alpha)} \simeq 1 - \frac{k^2}{2\alpha}, \tag{83}$$

and by resorting to Poisson identity we obtain

$$\begin{aligned}\frac{\beta F}{N} &= \beta\sum_{\mathbf{R}\neq 0} w(R) + \frac{\beta}{2}\delta_{\rm eff}^2\sum_{\mathbf{R}\neq 0}\nabla^2 w(R) \\ &\quad + \frac{\beta}{2\alpha}\sum_{\mathbf{R}\neq 0}\nabla^2 w(R) + \frac{\beta}{4\alpha}\delta_{\rm eff}^2\sum_{\mathbf{R}\neq 0}\nabla^2\nabla^2 w(R) \\ &\quad - \frac{1}{2}\ln\left[I_0\left(\frac{\beta}{v}\delta_{\rm eff}^2\lambda_{\rm eff}\right)\right] + G(\alpha,\nu) + \frac{\beta}{2}w(0) \\ &\quad - \frac{1}{2}\ln(2\pi),\end{aligned} \tag{84}$$

$$\lambda_{\rm eff} = v\sum_{\mathbf{R}}\left(\frac{\partial^2}{\partial x^2} - \frac{\partial^2}{\partial y^2}\right)\left[w(R) + \frac{1}{2\alpha}\nabla^2 w(R)\right]. \tag{85}$$

to be compared with Eqs. (36) and (42). In numerical calculations, Eqs. (84) and (85) have been chosen over Eqs. (81) and (82) for the same accuracy reasons explained in Sec. III B.

Equation (84) has been minimized numerically with respect to the lattice constant a and the additional parameters α, ν. The minimization with respect to a was carried out by direct evaluation of $\beta F/N$ via Brent's method [23]. At each minimization step, α and ν were determined by solving iteratively the equations $\partial F/\partial\alpha = \partial F/\partial\nu = 0$, whose expressions have been reported in Appendix C.

IV. MONTE CARLO

As stated in Sec. I, the mean-field method described above has been complemented by Monte Carlo simulations to study the behavior of the specific heat for $T \to 0$. The Monte Carlo code employed is largely based on the one we published in Ref. [18]. It performs a Metropolis [24] Monte Carlo (MC) simulation in the canonical ensemble. We have N particles disposed in $M \times M$ dimer units onto the sites of a regular triangular lattice within a parallelogram-shaped simulation cell. MC moves include single particle and dimer rigid translations, dimer rotations around their own center of mass, and modifications of the intradimer particle-particle distance. Moreover, we added angle moves, which allow for small changes of the cell angle, and aspect ratio moves, which alters the ratio between the height and the basis of the box, bounded to a fixed density value. All the amplitudes of such moves are tuned to obtain satisfactory acceptance ratios. Following Ref. [18], we have replaced the hard core of the HCGEM4 potential with a finite-amplitude repulsive potential as follows: $\varepsilon\exp[-(r/R)^4] + K$ for $r < \delta$, with $K = 5\varepsilon$, to have a regularized HCGEM4 potential. We have checked that, in the temperature range investigated, this does not change the

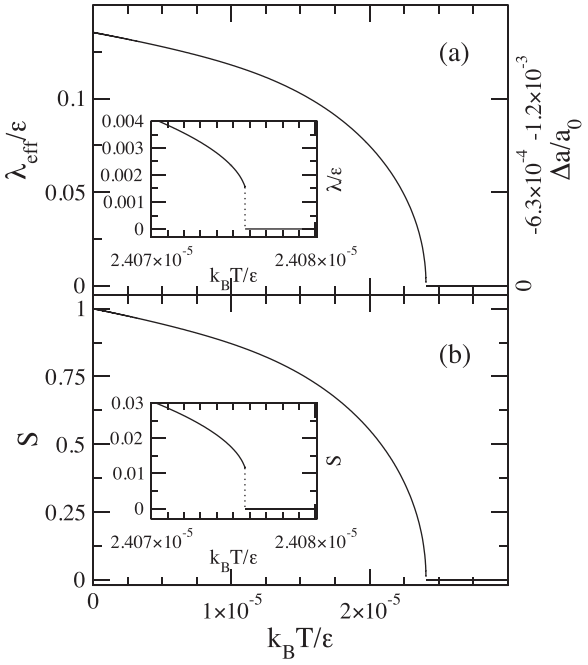

FIG. 4. Effective structural order parameter $\lambda_{\rm eff}$ (a) and nematic order parameter S (b) of the dimer crystal with dimer length $2\delta = 0.05R$ as a function of temperature. In panel (a), the right axis reports the relative difference $\Delta a/a_0$ of the lattice constant a with respect to the value $a_0 = 1.4234837R$ pertaining to the triangular lattice. In both panels, the inset is an enlargement of the transition region to make the discontinuity in the order parameter more conspicuous. The dotted line marks the discontinuity at the transition.

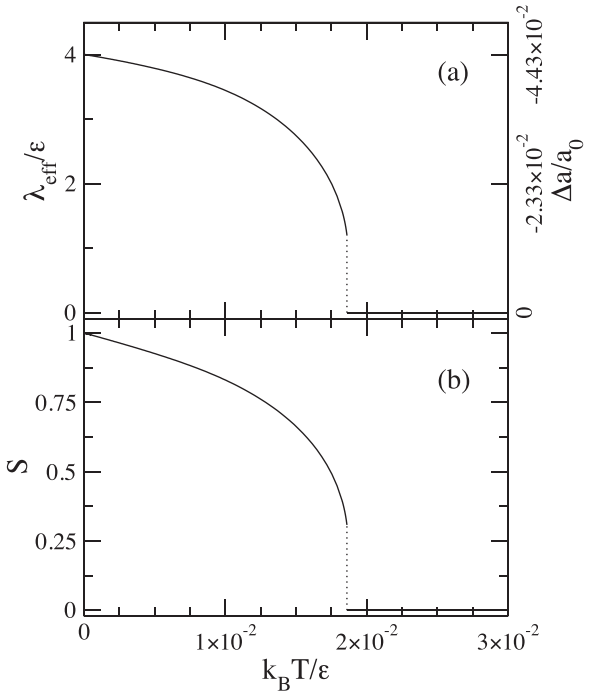

FIG. 5. Same as Fig. 4 for dimer length $2\delta = 0.25R$. Notice the much larger values of $\lambda_{\rm eff}$ and S at the transition compared to Fig. 4.

behavior of the system, since the configurations with mutually overlapping particles can safely be discarded. We have executed all simulations at the density $\rho = 1.13971R^{-2}$. Note that our code naturally exploits a simple MPI-parallelized approach on high-performance multiprocessor architectures.

V. RESULTS AND DISCUSSION

Here we present the results obtained by the numerical minimization of the Helmholtz free energy of Eq. (84). Figures 4 and 5 display the effective structural order parameter $\lambda_{\rm eff}$ and the nematic order parameter S for the cases $2\delta = 0.05R$ and $2\delta = 0.25R$ already considered in Figs. 1 and 2. The transition temperature T_0 amounts to $k_BT_0/\varepsilon = 2.4076 \times 10^{-5}$ for $2\delta = 0.05R$ and $k_BT/\varepsilon = 1.8600 \times 10^{-2}$ for $2\delta = 0.25R$, to be compared with the values reported in Sec. III C $k_BT_0/\varepsilon = 2.3893 \times 10^{-5}$ and $k_BT_0/\varepsilon = 1.5811 \times 10^{-2}$ in the absence of lattice sites and dimer length vibrations. Hence, the inclusion of these degrees of freedom leads to an increase of the transition temperature, which is mostly due to the fact that, because of the hard-core part of the intradimer interaction, the effective dimer length $\delta_{\rm eff}$ must necessarily exceed δ, see Eq. (80). Not surprisingly, the effect is stronger for longer dimers.

At any rate, T_0 remains much smaller than the temperature $T_\times$ of the transition from the fluid to the cluster crystal, as it should for the whole description to be consistent. $T_\times$ can be estimated from its value for a 2D fluid of particles interacting via a purely GEM4 potential with no hard core, since at the density $\rho = 1.13971R^{-2}$ considered here the packing fraction $\pi\rho\delta^2$ amounts to just $\simeq 2.2 \times 10^{-3}$ for $2\delta = 0.05R$ and $\simeq 5.6 \times 10^{-2}$ for $2\delta = 0.25R$, so the effect of the hard-core repulsion on $T_\times$ should be small. For $\rho = 1.13971R^{-2}$, a calculation similar to that carried out for a 3D GEM4 fluid in Ref. [5] gives $k_BT_\times/\varepsilon \simeq 0.2$. Hence, even for $2\delta = 0.25R$, $T_\times$ is more than one order of magnitude larger than T_0.

For both δ values, $\lambda_{\rm eff}$ and S have a similar behavior, and display the jump at T_0 which is the signature of a first-order transition. However, in line with the discussion of Sec. III C, for short dimers the first-order character of the transition is very weak, as testified by the very small size of the jump for $2\delta = 0.05R$.

According to Eqs. (57) and (58), based on the Landau expansion of the free energy, both λ at the transition and T_0 are proportional to δ^4 to leading order in δ. We expect a similar result to hold even in presence of lattice and dimer oscillations, provided λ and δ are replaced by $\lambda_{\rm eff}$ and $\delta_{\rm eff}$. This prediction has been tested in Fig. 6, where T_0 and $\lambda_{\rm eff}(T_0^-)$ have been plotted as a function of $\delta_{\rm eff}^4$ for several values of δ ranging between $0.05R$ and $0.25R$. Clearly, the prediction is satisfied within a very good accuracy. We checked that use of the effective quantities instead of the "bare" λ and δ considerably improves the agreement with the expected scaling, especially for longer dimers.

For $T \to 0$, the argument of $I_0(x)$ and $I_0'(x)$ in the expression of S goes to $+\infty$, see Eq. (40). In this limit, $I_0(x) \sim I_0'(x) \sim e^x/\sqrt{2\pi x}$, so that S goes to 1 irrespective of δ, as expected for perfect nematic order. In the same limit, one has $\lambda_{\rm eff} \sim \lambda$ but, at variance with S, the value reached by λ for $T \to 0$ is not the same for dimers of different length, since λ is basically a measure of the deviation Δa of the lattice constant

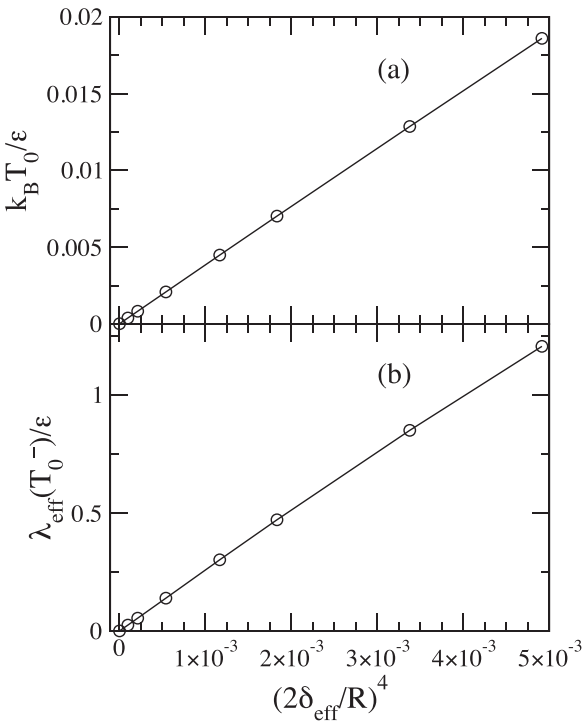

FIG. 6. Open circles: transition temperature T_0 (a) and effective order parameter at the transition $\lambda_{\rm eff}(T_0^-)$ (b) as a function of $(2\delta_{\rm eff})^4$, $2\delta_{\rm eff}$ being the effective dimer length. Notice the linear behavior of both T_0 and $\lambda_{\rm eff}(T_0^-)$. Lines are a guide for the eye.

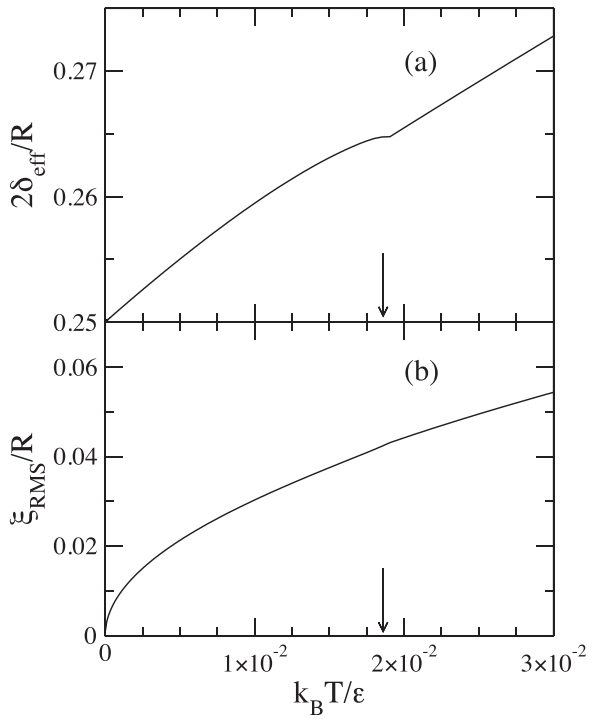

FIG. 7. Effective dimer length $2\delta_{\rm eff}$ (a) and root-mean-square displacement $\xi_{\rm RMS}$ of the dimer center from its equilibrium position (b) as a function of temperature for $2\delta = 0.25R$. The arrows mark the position of the transition temperature. Notice the kink of $\delta_{\rm eff}$ at the transition.

a from its value a_0 for the triangular lattice, whose extent increases on increasing δ, as can be appreciated by comparing the values of $\Delta a/a_0$ reported on the right axis of Figs. 4(a) and 5(a). We found that at small δ, λ is a linear function of a. As δ increases some deviations from linearity appear which, however, remain small.

At $T = 0$, the mean-field free energy of Eq. (17), with no quadrupole approximation, gives the exact potential energy U of the perfectly ordered nematic state. By comparing the lattice constant and the potential energy obtained by the present calculation at $T = 0$ with the exact calculation of Ref. [18], we can obtain an assessment of the accuracy of the quadrupole approximation used here. The comparison is made in Table I for $2\delta = 0.05R$ and $2\delta = 0.25R$. Clearly, the discrepancies are larger for the longer dimers, but even in that case are still below 1%.

As stated in Sec. III E, the treatment of the degrees of freedom describing the dimer position and length assumes that these quantities deviate little from their equilibrium values. To check this assumption, in Fig. 7 we have plotted the effective dimer length $\delta_{\rm eff}$ and the root mean square displacement $\xi_{\rm RMS} = 1/\sqrt{\alpha}$ of the dimer center from its equilibrium position as a function of temperature for $2\delta = 0.25R$. The larger deviations are observed for $\delta_{\rm eff}$, but still $(\delta_{\rm eff} - \delta)/\delta$ does not exceed 6% at the transition. For shorter dimers, the deviations are even smaller: for $2\delta = 0.05R$, we find $(\delta_{\rm eff} - \delta)/\delta \simeq 0.2\%$ at the transition. We also note that the transition manifests in a small kink in the plot of $\delta_{\rm eff}$, whereas it is hardly detectable in the plot of $\xi_{\rm RMS}$.

TABLE I. Exact lattice constant a and potential energy per particle U/N at $T = 0$ and corresponding values predicted by the quadrupole approximation for $2\delta = 0.05R$ and $2\delta = 0.25R$.

$2\delta/R$	$(a/R)_{\rm exact}$	$(a/R)_{\rm quad}$	$U/(N\varepsilon)_{\rm exact}$	$U/(N\varepsilon)_{\rm quad}$
0.05	1.4211105	1.4210841	0.6019478	0.6019481
0.25	1.3729536	1.3603179	0.6701436	0.6679406

We now turn to the discussion of the configurational specific heat per particle c_V. In Figs. 8 and 9 c_V has been plotted as a function of temperature for $2\delta = 0.05R$ and $2\delta = 0.25R$ respectively. Unlike in the situation considered in Sec. III C, where only the rotational degrees of freedom of the dimers were taken into account, now there is a contribution to c_V due to lattice and dimer vibrations, so that c_V is not zero even above the transition temperature T_0. Aside of that, the overall qualitative behavior of c_V at the transition is the same. At T_0, c_V exhibits the expected discontinuity, featuring a peak for $T \to T_0^-$. For $2\delta = 0.05R$ the peak is extremely sharp, although the enlargement of the peak region displayed in the inset to Fig. 8 shows that c_V remains regular all the way up to the discontinuity. For longer dimers the peak behaves more smoothly, as evidenced in Fig. 9.

The only instance in which we found the inclusion of lattice and dimer vibrations to entail a qualitative difference with respect to the dimer crystal with purely rotational degrees of freedom concerns the discontinuity of $\Delta c_V \equiv c_V(T_0^-) - c_V(T_0^+)$, which according to Eq. (60) is predicted to behave

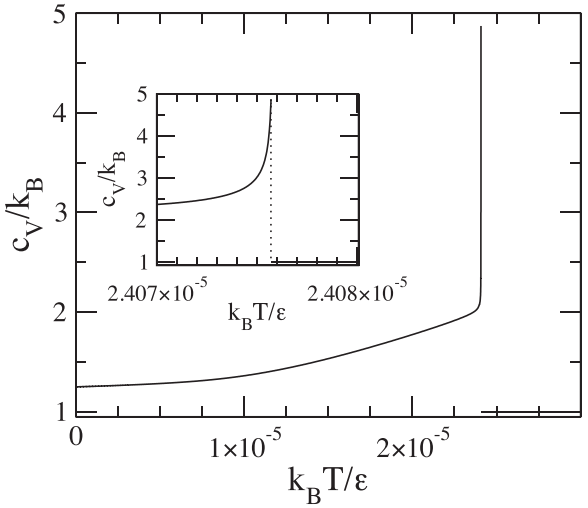

FIG. 8. Configurational specific heat at constant volume c_V of the dimer crystal with dimer length $2\delta = 0.05R$ as a function of temperature. The inset is an enlargement of the transition region. The dotted line marks the discontinuity of c_V at the transition.

as $\Delta c_V \sim 4k_B + \mathcal{O}(\delta^4)$ for $\delta \to 0$. This prediction is tested in Fig. 10 both with and without the additional lattice and dimer degrees of freedom. Figure 10(a) shows that, when only rotational degrees of freedom are present, Δc_V does tend to $4k_B$ for $\delta \to 0$, and that in this limit it behaves linearly when plotted as a function δ^4. However, this is no longer true when lattice and dimer vibrations are taken into account: in that case, Δc_V is not a linear function of $\delta_{\rm eff}^4$, nor of δ^4 for that matter. Clearly, the inclusion of these degrees of freedom must imply the presence of additional contributions to Δc_V, which affect its dependence on δ. In this respect we observe that, unlike the internal energy, c_V depends explicitly on the derivatives of the variational parameters α and ν with respect to T, and that the kink in the plot of $\delta_{\rm eff}$ as a function of T observed in Fig. 7 indicates a discontinuity of $d\delta_{\rm eff}/dT$ and consequently of $d\nu/dT$ at the transition. We did not pursue an analytical study of Δc_V similar to that carried out in Sec. III C for the crystal with only rotational degrees of

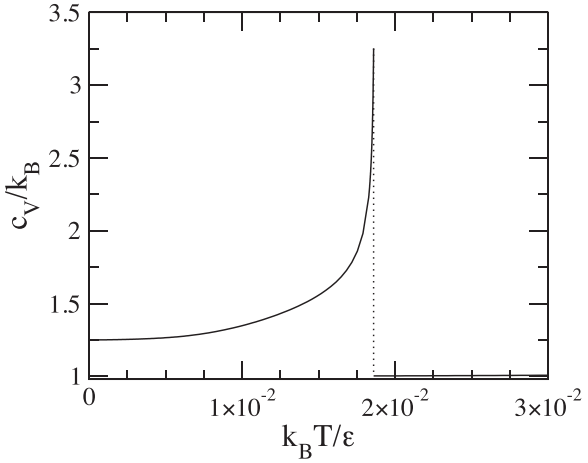

FIG. 9. Same as Fig. 8 for dimer length $2\delta = 0.25R$.

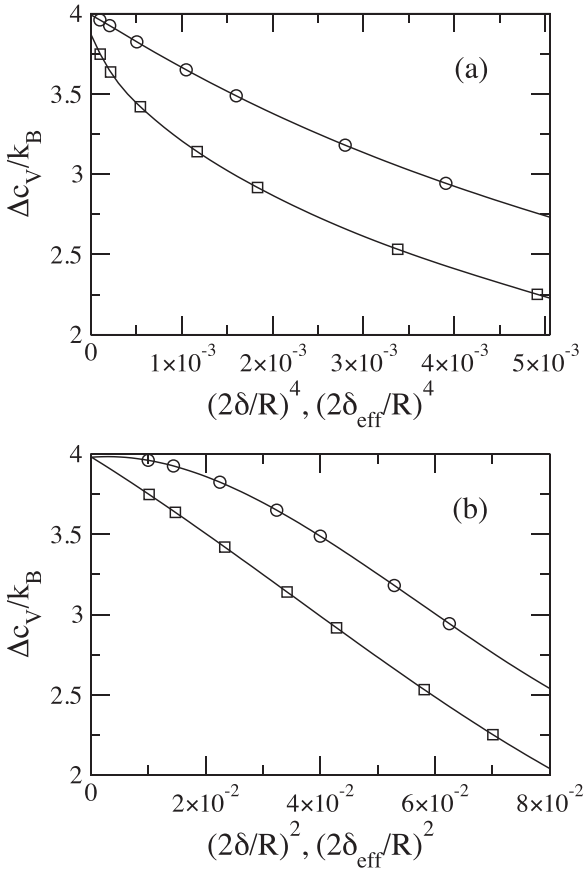

FIG. 10. (a) Discontinuity of the specific heat at constant volume $\Delta c_V \equiv c_V(T_0^-) - c_V(T_0^+)$ at the transition for the dimer crystal with fixed positions of the dimer centers and dimer length as a function of $(2\delta)^4$ (circles), and with the inclusion of lattice and dimer length vibrations as a function of $(2\delta_{\rm eff})^4$ (squares). The lines are cubic splines interpolating the data points. (b) Same as panel (a), but as a function of $(2\delta)^2$ (circles) and $(2\delta_{\rm eff})^2$ (squares).

freedom, but Fig. 10(b) strongly suggests that, when lattice and dimer length vibrations are considered, Δc_V behaves as a linear function of $\delta_{\rm eff}^2$, and that for $\delta \to 0$ the limit $4k_B$ is recovered. We also note that in both cases Δc_V is a decreasing function of δ, so that the peak of c_V decreases on increasing δ, as could be surmised by comparing Figs. 8 and 9.

A feature of c_V which is not directly related to the transition, but nevertheless should be addressed, concerns its low-temperature behavior. Figures 8 and 9 show that for $T \to 0$, c_V reaches the value $1.25\,k_B$. This is corroborated by MC simulations performed at $k_BT/\varepsilon = 10^{-6}$, 7.5×10^{-7}, 5×10^{-7}, 2.5×10^{-7}, 10^{-7}, each consisting of 2.5×10^6 steps, after as many devoted to equilibration. The comparison between the theoretical and simulation predictions for c_V is shown in Fig. 11, which displays an expanded view of the low-temperature region in semi-logarithmic scale. Despite the slight offset between the theoretical and the simulation data, simulations are fully consistent with c_V saturating at $1.25\,k_B$ for $T \to 0$.

The above result is at odd with the equipartition principle, according to which each configurational degree of freedom should contribute $k_B/2$ to the thermal capacity at constant

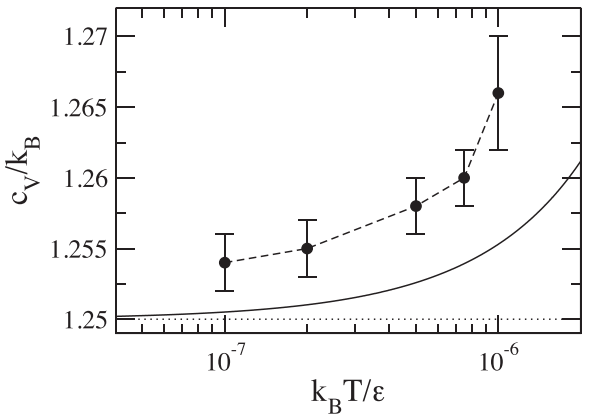

FIG. 11. Configurational specific heat at constant volume c_V for dimer length $2\delta = 0.05R$ in the low-temperature region, with T in logarithmic scale. Solid curve: theoretical prediction. Dots: MC simulation. The dashed curve is a guide for the eye. The errorbars are obtained from blocking the data in five groups of 5×10^5 MC steps each. The dotted line marks the limiting value $1.25\,k_B$ for $T \to 0$.

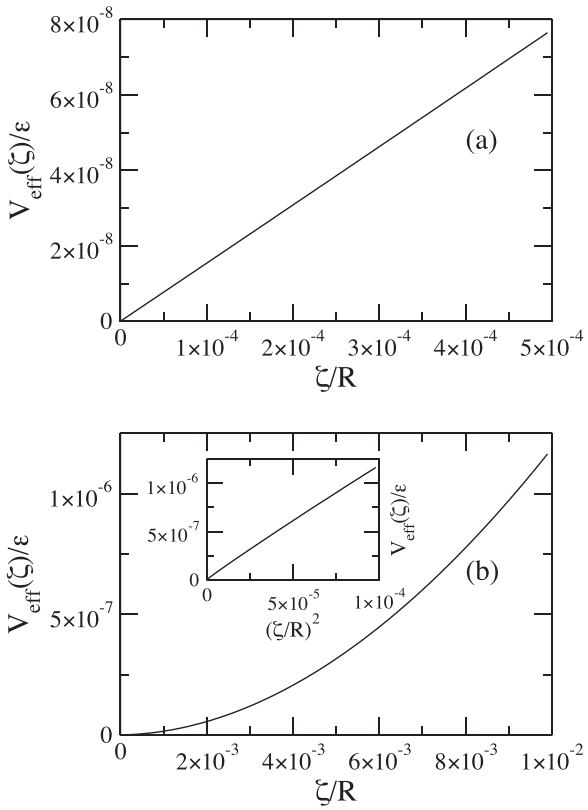

FIG. 12. (a) Effective separation potential of a dimer $V_{\rm eff}(\zeta)$ as a function of the difference ζ between the separation of the dimer particles and the separation at equilibrium for the HCGEM4 potential considered in this paper. (b) Same as panel (a) for the smooth-core SCGL6 potential. For the HCGEM4 potential, $V_{\rm eff}(\zeta)$ is a linear function of ζ, whereas for the SCGL6 potential it is a quadratic function of ζ, as evidenced by the linear behavior of $V_{\rm eff}(\zeta)$ when plotted as a function of ζ^2 displayed in the inset to panel (b).

volume, thereby giving a configurational specific heat equal to k_B in a two-dimensional crystal with two positional degrees of freedom per particle. In the present situation particles are arranged into dimers, resulting in four degrees of freedom per dimer. Of course, the degrees of freedom describing the normal modes do not correspond to the positions of the individual particles of the dimer. Rather, two of them specify the position $\boldsymbol{\xi}$ of the dimer center, one gives the distance η between the dimer particles, and the remaining one fixes the dimer orientation ϑ in the plane. Still, this should have no effect on the final result, since the total number of degrees of freedom remains unchanged, leading to $4 \times k_B/2 = 2\,k_B$ for the specific heat per dimer, i.e., to k_B for the specific heat per particle. One may then wonder where the extra $0.25\,k_B$ comes from.

To clarify the origin of the anomaly, we determined numerically the effective separation potential of a dimer: we picked up a dimer at random in the simulation box and, while keeping the remaining $N-2$ particles frozen, progressively separated its particles along the direction of the nematic director, so that their mutual distance exceeds the equilibrium distance 2δ by ζ. We then measured the difference $V_{\rm eff}(\zeta) = U(\zeta) - U_0$ between the total potential energy U of the system, and the potential energy at equilibrium U_0. The resulting $V_{\rm eff}(\zeta)$ is plotted in Fig. 12(a), and is clearly a linear function of ζ, instead of being a quadratic function as generally expected. This behavior is due to the hard-core part of the interaction, which implies that, as soon as $\zeta \neq 0$, the restoring force between the two dimer particles jumps to a finite value, instead of increasing continuously from 0.

As a consequence, the contribution Z to the partition function due to the intradimer separation has the form

$$Z = \int_0^{+\infty} d\zeta(\zeta + 2\delta)e^{-\beta u\zeta} = \left(\frac{k_BT}{u}\right)^2 + 2\delta\,\frac{k_BT}{u}, \quad (86)$$

where we have set $V_{\rm eff}(\zeta) = u\,\zeta$, u being a constant. At low temperature, this expression behaves as $Z \sim k_BT$, giving a contribution to c_V equal to k_B, twice that obtained for a quadratic $V_{\rm eff}$. Therefore, we have the following dimer contributions to the specific heat: $k_B/2 + k_B/2$ from the translational degrees of freedom, $k_B/2$ from the orientational degree of freedom, and k_B from to the dimer length degree of freedom, resulting in $2.5\,k_B$ per dimer, i.e., $1.25\,k_B$ per particle.

This picture is in agreement with the study of the theoretical c_V presented in Appendix D, where the low-temperature limit $1.25\,k_B$ is obtained analytically, and the anomaly is traced back to the dimer length fluctuations described by the probability distribution $p_L(\eta)$, with η half the dimer length. The exponential form $p_L(\eta) \sim e^{-\gamma(\eta-\delta)}$ of Eq. (75) was preferred to a Gaussian, because we deemed it more appropriate to describe the linear dependence of $V_{\rm eff}$ on the dimer stretching $\zeta = 2(\eta - \delta)$. Indeed, we checked that a Gaussian $p_L(\eta) \sim e^{-\gamma'(\eta-\delta)^2}$ leads to an increase of the Helmholtz free energy. At the same time, we should point out that the anomaly of c_V does not hinge on the *ansatz* of Eq. (75) for $p_L(\eta)$. In fact, having $p_L(\eta)$ assume a Gaussian form would imply that, at low temperature, the Gaussian width parameter γ' would scale as $\gamma' \sim \beta^2$, at variance with the dependence $\gamma \sim \beta$ obtained in the same limit with the present $p_L(\eta)$; see Appendix C. This is also different from the scaling $\alpha \sim \beta$ of

the width α of the Gaussian which describes the oscillations of the dimer center according to Eq. (74). As a result, the contribution to the specific heat per dimer due to the dimer length fluctuations would still amount to k_B, as is found here. Therefore, the specific form of $p_L(\eta)$ is not crucial to recover the anomaly of c_V within the present description. What really matters to that end, is that the potential energy obtained from Eq. (84) at low temperature is a linear, rather than quadratic, function of the deviation of the dimer length from its equilibrium value 2δ. This holds irrespective of δ, except in the trivial case $\delta = 0$.

In Ref. [18] we considered also a pair potential referred to as "smooth core plus generalized Lorentzian with exponent 6" (SCGL6) originally introduced in Ref. [25], which again gives dimer formation and a nematic state at low temperature, but where the hard core is replaced by a smooth repulsion diverging as $\sim 1/r^6$ for $r \to 0$. Figure 12(b) displays V_{eff} for the SCGL6 interaction: in that case, V_{eff} has the usual quadratic dependence on ζ, leading to $Z \sim \sqrt{k_B T}$ at low temperature and to the expected contribution to c_V equal to $k_B/2$. Indeed, the MC simulation of a dimer crystal of particles interacting via the SCGL6 potential gives $c_V \to k_B$ for $T \to 0$, in agreement with equipartition [26].

With hindsight, the anomalous behavior of c_V displayed in Figs. 8 and 9 is somewhat deceptive, because above the transition temperature T_0, where there is no contribution from the rotational degrees of freedom, c_V assumes the value k_B expected on the basis of equipartition. One might then be led to attribute the anomaly to the onset of nematic ordering below T_0, where rotational degrees of freedom contribute to c_V. Instead, the rotational contribution does fulfill equipartition, and the anomaly is already there above T_0, where the apparently regular value k_B, i.e., $2\,k_B$ per dimer, is in fact due to just three dimer degrees of freedom.

VI. CONCLUSIONS

We have presented a mean-field theory to describe the occurrence of orientational order in a 2D crystal of dimers resulting from association of particles interacting via a hard-core–soft-shell potential. In the model discussed here the soft shell consists of a GEM4 interaction, but the same analysis would hold for any $Q^{\pm}$ interaction other than the GEM4.

According to the present description, at a temperature much lower than that at which the crystal forms, the system undergoes a structural transition from the triangular lattice, where the dimers display no orientational order, to the centered rectangular lattice, where the dimers form a nematic phase. Hence, the structural and orientational transitions coincide, as evidenced by the mutual dependence of their order parameters brought forth by this treatment.

The transition is of first-order type, similarly to that from the isotropic to the nematic phase in liquid crystals. This is reflected in the appearance of a cubic term in the Landau expansion of the free energy in powers of the order parameter. However, unlike in liquid crystals, not every direction of nematic order is equally acceptable. In fact, the nematic director can assume only a discrete set of orientations: specifically, those orthogonal to the three possible directions along which the lattice may shrink, to turn from triangular to centered rectangular. Moreover, the first-order character of the transition is very weak, especially for large shell-to-core ratio. In this regime the discontinuity of the order parameter is so small, that it would be probably very difficult to distinguish this transition from a second-order one, both in experiments and in simulations.

The theory has also been generalized to account for lattice vibrations and fluctuations of the distance between the dimer particles. Formally, this is achieved by introducing an effective order parameter and an effective dimer length, and does not lead to significant differences in the qualitative picture of the transition. The most notable effect entailed by the inclusion of these degrees of freedom concerns the behavior of the specific heat c_V in the nematic phase in the $T \to 0$ limit, which we have studied also by MC simulations. Simulation and theory agree in predicting that, in this limit, the contribution of each dimer to c_V exceeds by $k_B/2$ the value expected on the basis of the equipartition principle. This is due to the fact that, because of the singular hard-core part of the interaction, the potential energy of the dimer is not a quadratic function of its length. Of course, we should keep in mind that the above result is based on a classical calculation. According to it, for the anomaly in c_V to become evident one has to move below the transition temperature T_0, where quantum effects might be relevant in actual systems.

Recently, dendrimers interacting via $Q^{\pm}$ potentials have been synthesized, and the formation of cluster crystals in solutions of such dendrimers has been observed experimentally [27]. In 2D, systems of superparamagnetic particles trapped in a thin cell have been shown to provide an experimental realization of the hard-core–soft-shell interaction, leading to a host of different mesophases [28]. One may then ask whether the transition described here would be detectable in these systems.

In this respect, its very low temperature represents a major hindrance: as discussed in Sec. V, even for the longest dimers which we considered, such that $2\delta = 0.25R$, T_0 is more than one order of magnitude smaller than the temperature at which the dimer crystal forms. Given that in both systems mentioned above the particles are dispersed in water, freezing of the solvent would intervene well before T_0 is reached, even assuming that the crystal can be realized at temperatures at which the solvent is still liquid. T_0 could be increased by considering even longer dimers, hence further decreasing the shell-to-core ratio, but besides the fact that in this regime the quadrupole approximation used here would become inaccurate, one has to take into account that at small shell-to-core ratios the system would probably not form dimers at all, as evidenced in the study of minimum energy configurations of the hard-core–square shoulder potential [13,14]. In light of the above considerations, soft-matter cluster crystals are unlikely to lend themselves to the experimental observation of dimer nematic ordering, or the related structural transition.

Nevertheless, there are other systems belonging to the realm of atomic or molecular crystals where these effects could be detected. As mentioned in Sec. III D, a scenario very similar to that considered here occurs in the antiferromagnetic transition of $Fe_{1/3}NbS_2$ studied in Ref. [22]. This compound features planes of Fe atoms arranged on a triangular lattice intercalating between NbS_2 planes. Despite the

antiferromagnetic coupling between neighboring Fe atoms, the frustration due to the triangular lattice would prevent the onset of a magnetically ordered state. However, below the Néel temperature $T_N = 43\,\mathrm{K}$ the lattice experiences a deformation along one of the three directions of the Fe-Fe bonds, which relieves the frustration and leads to an antiferromagnetic phase via a first-order transition. The atomic spins are mainly oriented along the direction perpendicular to the lattice planes, but they still present a small in-plane component which, interestingly, undergoes an isotropic-nematic transition at T_N. This in-plane component of the spins plays then the role of the dimers in the system considered here.

Another class of materials which is more closely related to the present model and could display the same kind of transition is represented by plastic crystals. Indeed, irrespective of the details of the mechanism which leads to dimer formation, our system can be regarded as a simple model of a 2D plastic crystal. Generally, when plastic crystals are cooled their orientational degrees of freedom eventually freeze forming a disordered, glassy-like arrangement [29]. It would be interesting to investigate if 2D films of plastic crystals could present a transition to an ordered nematic phase via a mechanism similar to that which we have discussed.

In this paper the main emphasis was given to the discussion of the theory, with little contribution from simulations. A more extended comparison between the simulation results and the theoretical predictions involving both thermodynamic and structural quantities will be presented in the future.

ACKNOWLEDGMENTS

D.P. acknowledges support by Università degli Studi di Milano, Project No. PSR2022_DIP_008-Linea 2.

APPENDIX A: DERIVATIVES OF THE LATTICE SUM WITH RESPECT TO THE ORDER PARAMETER λ

Here we report the expressions of the second, third, and fourth derivatives of the lattice sum $\mathcal{F}$ defined in Eq. (44) with respect to λ evaluated on the triangular lattice such that $\lambda = 0$. We start from Eqs. (47) and (48), which we rewrite below for completeness:

$$S_1[g] = \sum_{\mathbf{k}} \left(k_y^2 - k_x^2\right) g(k), \tag{A1}$$

$$S_2[g] = \sum_{\mathbf{k}} \left[\left(k_y^2 - k_x^2\right)^2 \frac{dg(k)}{d(k^2)} + k^2 g(k) \right]. \tag{A2}$$

These are generalized via the recurrence relation

$$S_n[g] = \frac{a}{2} \frac{d}{da} S_{n-1}[g], \tag{A3}$$

thereby yielding

$$S_3[g] = \sum_{\mathbf{k}} \left[\left(k_y^2 - k_x^2\right)^3 \frac{d^2 g(k)}{d(k^2)^2} + \left(k_y^2 - k_x^2\right) \left(3k^2 \frac{dg(k)}{d(k^2)} + g(k) \right) \right], \tag{A4}$$

$$S_4[g] = \sum_{\mathbf{k}} \left[\left(k_y^2 - k_x^2\right)^4 \frac{d^3 g(k)}{d(k^2)^3} + 2\left(k_y^2 - k_x^2\right)^2 \times \left(3k^2 \frac{d^2 g(k)}{d(k^2)^2} + 2\frac{dg(k)}{d(k^2)} \right) + k^2 \left(3k^2 \frac{dg(k)}{d(k^2)} + g(k) \right) \right]. \tag{A5}$$

A tedious but straightforward calculation gives for the higher-order derivatives of $\mathcal{F}$

$$\left.\frac{d^2\mathcal{F}}{d\lambda^2}\right|_{\lambda=0} = S_2\left[\frac{df}{d(k^2)}\right] \frac{1}{\{S_2[\widetilde{w}]\}^2}, \tag{A6}$$

$$\left.\frac{d^3\mathcal{F}}{d\lambda^3}\right|_{\lambda=0} = \left\{ S_2[\widetilde{w}]\, S_3\left[\frac{df}{d(k^2)}\right] - 3S_3[\widetilde{w}]\, S_2\left[\frac{df}{d(k^2)}\right] \right\} \times \frac{1}{\{S_2[\widetilde{w}]\}^4}, \tag{A7}$$

$$\left.\frac{d^4\mathcal{F}}{d\lambda^4}\right|_{\lambda=0} = \left\{ \{S_2[\widetilde{w}]\}^2 S_4\left[\frac{df}{d(k^2)}\right] - 6S_2[\widetilde{w}] S_3[\widetilde{w}]\, S_3\left[\frac{df}{d(k^2)}\right] - 4S_2[\widetilde{w}] S_4[\widetilde{w}]\, S_2\left[\frac{df}{d(k^2)}\right] + 15\{S_3[\widetilde{w}]\}^2 S_2\left[\frac{df}{d(k^2)}\right] \right\} \frac{1}{\{S_2[\widetilde{w}]\}^6}, \tag{A8}$$

where $f(k)$ is given by Eq. (44), and it is understood that all functionals S_n are calculated on the triangular lattice.

APPENDIX B: DERIVATIVES OF THE FREE ENERGY WITH RESPECT TO μ

Here we determine the first and second derivatives of the Helmholtz free energy F with respect to the variable μ defined in Eq. (61) evaluated at $\mu = 0$. According to Eq. (35), the lattice-dependent part of F contains the lattice sum $\mathcal{F} = \sum_{\mathbf{k}} f(k)$ defined in Eq. (44), and the logarithmic term $\ln[\, I_0(\beta\delta^2\Lambda/v)\,]$, with $\Lambda = \pm\sqrt{\lambda^2 + \mu^2}$. The derivatives with respect to μ of the latter contribution are obtained straightforwardly. Let us then focus on the derivatives of $\mathcal{F}$. We first consider the derivatives with respect to the variables a and s which determine the matrix of the primitive vectors given by Eq. (19).

The derivative of $\mathcal{F}$ with respect to the lattice constant a has already been determined in Eqs. (46) and (47). The derivative with respect to s of the wave vector $\mathbf{k}$ is given by

$$\frac{\partial}{\partial s}\begin{pmatrix} k_x \\ k_y \end{pmatrix} = \frac{\partial \mathbf{B}}{\partial s}\, \mathbf{B}^{-1} \begin{pmatrix} k_x \\ k_y \end{pmatrix} = -\frac{a^2}{v}\begin{pmatrix} 0 \\ k_x \end{pmatrix}. \tag{B1}$$

This yields

$$\frac{\partial \mathcal{F}}{\partial s} = -\frac{2a^2}{v}\, Q_1\left[\frac{df}{d(k^2)}\right], \tag{B2}$$

where the functional Q_1 is defined by

$$Q_1[g] = \sum_{\mathbf{k}} k_x k_y\, g(k). \tag{B3}$$

The derivatives with respect to λ and μ can be determined via the relation

$$\begin{pmatrix} \frac{\partial \mathcal{F}}{\partial \lambda} \\ \frac{\partial \mathcal{F}}{\partial \mu} \end{pmatrix} = \begin{pmatrix} \frac{\partial \lambda}{\partial a} & \frac{\partial \mu}{\partial a} \\ \frac{\partial \lambda}{\partial s} & \frac{\partial \mu}{\partial s} \end{pmatrix}^{-1} \begin{pmatrix} \frac{\partial \mathcal{F}}{\partial a} \\ \frac{\partial \mathcal{F}}{\partial s} \end{pmatrix}, \tag{B4}$$

where $\partial\lambda/\partial a$ is given by Eq. (46), and the remaining derivatives $\partial\lambda/\partial s$, $\partial\mu/\partial a$, $\partial\mu/\partial s$ are similarly determined by the definitions of λ and μ in Eqs. (41) and (61) via Eqs. (45) and (B1). This gives

$$\begin{pmatrix} \frac{\partial \mathcal{F}}{\partial \lambda} \\ \frac{\partial \mathcal{F}}{\partial \mu} \end{pmatrix} = \frac{1}{BG - CE} \begin{pmatrix} G & -C \\ -E & B \end{pmatrix} \begin{pmatrix} S_1\left[\frac{df}{d(k^2)}\right] \\ Q_1\left[\frac{df}{d(k^2)}\right] \end{pmatrix}, \tag{B5}$$

where the functional S_1 is defined in Eq. (A1), the quantity B coincides with $S_2[\widetilde{w}]$, S_2 being the functional defined in Eq. (A2), and the quantities C, E, G are given by

$$C = \sum_{\mathbf{k}} 2k_x k_y \left(k_y^2 - k_x^2\right) \frac{d\widetilde{w}(k)}{d(k^2)}, \tag{B6}$$

$$E = \sum_{\mathbf{k}} k_x k_y \left[\left(k_y^2 - k_x^2\right) \frac{d\widetilde{w}(k)}{d(k^2)} + \widetilde{w}(k) \right], \tag{B7}$$

$$G = \sum_{\mathbf{k}} k_x^2 \left[2k_y^2 \frac{d\widetilde{w}(k)}{d(k^2)} + \widetilde{w}(k) \right]. \tag{B8}$$

For a centered rectangular lattice whose unit cell sides lie along the x and y axes, one has $Q_1[g] = C = E = 0$. Equation (B5) then gives back Eq. (49) for $\partial\mathcal{F}/\partial\lambda$, whereas for $\partial\mathcal{F}/\partial\mu$ we find

$$\frac{\partial \mathcal{F}}{\partial \mu} = \frac{1}{G} Q_1\left[\frac{df}{d(k^2)}\right] = 0. \tag{B9}$$

To determine the second derivatives, we replace $\mathcal{F}$ in Eq. (B4) with $\partial\mathcal{F}/\partial\mu$ to obtain

$$\begin{pmatrix} \frac{\partial^2 \mathcal{F}}{\partial \lambda \partial \mu} \\ \frac{\partial^2 \mathcal{F}}{\partial \mu^2} \end{pmatrix} = \begin{pmatrix} \frac{\partial \lambda}{\partial a} & \frac{\partial \mu}{\partial a} \\ \frac{\partial \lambda}{\partial s} & \frac{\partial \mu}{\partial s} \end{pmatrix}^{-1} \begin{pmatrix} \frac{\partial^2 \mathcal{F}}{\partial a \partial \mu} \\ \frac{\partial^2 \mathcal{F}}{\partial s \partial \mu} \end{pmatrix}. \tag{B10}$$

To simplify the notation, we introduce the differential operators $\partial/\partial u$ and $\partial/\partial t$ defined as follows: we consider a lattice-dependent quantity $\mathcal{G}$ of the form $\mathcal{G} = \sum_{\mathbf{k}} g(\mathbf{k})$. We then express the derivatives of $\mathcal{G}$ with respect to a and s as

$$\frac{\partial \mathcal{G}}{\partial a} = -\frac{2}{a} \frac{\partial \mathcal{G}}{\partial u}, \quad \frac{\partial \mathcal{G}}{\partial s} = -\frac{a^2}{v} \frac{\partial \mathcal{G}}{\partial t}, \tag{B11}$$

where we have set

$$\frac{\partial \mathcal{G}}{\partial u} = \frac{1}{2} \sum_{\mathbf{k}} \left(k_x \frac{\partial}{\partial k_x} - k_y \frac{\partial}{\partial k_y} \right) g(\mathbf{k}), \tag{B12}$$

$$\frac{\partial \mathcal{G}}{\partial t} = \sum_{\mathbf{k}} k_x \frac{\partial g(\mathbf{k})}{\partial k_y}. \tag{B13}$$

We now take $\partial\mathcal{F}/\partial\mu$ given by Eq. (B5), differentiate it with respect to a and s via Eqs. (B11)–(B13), and insert the result into Eq. (B10) to obtain

$$\begin{aligned} \frac{\partial^2 \mathcal{F}}{\partial \lambda \partial \mu} = \frac{1}{BG - CE} \Bigg\{ & G \left[\frac{\partial}{\partial u} \left[\frac{1}{BG - CE} (E \ -B) \right] \begin{pmatrix} S_1 \\ Q_1 \end{pmatrix} + \frac{1}{BG - CE} (E \ -B) \begin{pmatrix} \frac{\partial S_1}{\partial u} \\ \frac{\partial Q_1}{\partial u} \end{pmatrix} \right] \\ & + \frac{C}{2} \left[\frac{\partial}{\partial t} \left[\frac{1}{BG - CE} (E \ -B) \right] \begin{pmatrix} S_1 \\ Q_1 \end{pmatrix} + \frac{1}{BG - CE} (E \ -B) \begin{pmatrix} \frac{\partial S_1}{\partial t} \\ \frac{\partial Q_1}{\partial t} \end{pmatrix} \right] \Bigg\}, \end{aligned} \tag{B14}$$

$$\begin{aligned} \frac{\partial^2 \mathcal{F}}{\partial \mu^2} = \frac{1}{BG - CE} \Bigg\{ & -E \left[\frac{\partial}{\partial u} \left[\frac{1}{BG - CE} (E \ -B) \right] \begin{pmatrix} S_1 \\ Q_1 \end{pmatrix} + \frac{1}{BG - CE} (E \ -B) \begin{pmatrix} \frac{\partial S_1}{\partial u} \\ \frac{\partial Q_1}{\partial u} \end{pmatrix} \right] \\ & - \frac{B}{2} \left[\frac{\partial}{\partial t} \left[\frac{1}{BG - CE} (E \ -B) \right] \begin{pmatrix} S_1 \\ Q_1 \end{pmatrix} + \frac{1}{BG - CE} (E \ -B) \begin{pmatrix} \frac{\partial S_1}{\partial t} \\ \frac{\partial Q_1}{\partial t} \end{pmatrix} \right] \Bigg\}, \end{aligned} \tag{B15}$$

where it is understood that the functionals S_1, Q_1 and their derivatives are evaluated at $df/d(k^2)$ as in Eq. (B5). By taking again into account the relation $Q_1[g] = C = E = 0$ which holds for the centered rectangular lattice, Eq. (B14) simplifies to

$$\left.\frac{\partial^2 \mathcal{F}}{\partial \lambda \partial \mu}\right|_{\lambda,0} = \frac{1}{BG} \left(\frac{S_1}{B} \frac{\partial E}{\partial u} - \frac{\partial Q_1}{\partial u} \right). \tag{B16}$$

By applying $\partial/\partial u$ defined in Eq. (B12) to Q_1 and E given respectively by Eqs. (B3) and (B7), it is found that for the centered rectangular lattice both $\partial E/\partial u$ and $\partial Q_1/\partial u$ vanish. We then have

$$\left.\frac{\partial^2 \mathcal{F}}{\partial \lambda \partial \mu}\right|_{\lambda,0} = 0. \tag{B17}$$

Similarly, Eq. (B15) becomes

$$\left.\frac{\partial^2 \mathcal{F}}{\partial \mu^2}\right|_{\lambda,0} = \frac{1}{2G^2} \left(-\frac{S_1}{B} \frac{\partial E}{\partial t} + \frac{\partial Q_1}{\partial t} \right), \tag{B18}$$

which, unlike Eq. (B16), does not vanish, since neither $\partial E/\partial t$ nor $\partial Q_1/\partial t$ do. Specifically, we get

$$\frac{\partial Q_1}{\partial t} = \sum_{\mathbf{k}} k_x^2 \left[\frac{df(k)}{d(k^2)} + 2k_y^2 \frac{d^2 f(k)}{d(k^2)^2} \right], \tag{B19}$$

$$\begin{aligned} \frac{\partial E}{\partial t} = \sum_{\mathbf{k}} k_x^2 \Bigg[& \widetilde{w}(k) + \left(5k_y^2 - k_x^2\right) \frac{d\widetilde{w}(k)}{d(k)^2} \\ & + 2k_y^2 \left(k_y^2 - k_x^2\right) \frac{d^2 \widetilde{w}(k)}{d(k^2)^2} \Bigg]. \end{aligned} \tag{B20}$$

By adding to $\mathcal{F}$ the logarithmic term $\ln[\, I_0(\beta\delta^2\Lambda/v)\,]$, we finally obtain for the derivatives of the Helmholtz free energy per particle F/N evaluated at $\mu = 0$

$$\frac{\partial^2}{\partial\lambda\partial\mu}\left(\frac{F}{N}\right)_{\lambda,0} = 0, \tag{B21}$$

$$\frac{\partial^2}{\partial\mu^2}\left(\frac{F}{N}\right)_{\lambda,0} = \frac{1}{v}\left[\left.\frac{\partial^2\mathcal{F}}{\partial\mu^2}\right|_{\lambda,0} - \frac{\delta^2}{2|\lambda|}\frac{I_0'\left(\frac{\beta}{v}\delta^2|\lambda|\right)}{I_0\left(\frac{\beta}{v}\delta^2|\lambda|\right)}\right]. \tag{B22}$$

APPENDIX C: DERIVATIVES OF THE FREE ENERGY WITH RESPECT TO THE VARIATIONAL PARAMETERS α, ν

Here we report the equations for the variational parameters α, $\nu = \gamma\delta$ which determine the probability distributions respectively of the position of the dimer center and of the dimer length according to Eqs. (74) and (75).

We differentiate Eq. (81) for the Helmholtz free energy F with respect to α and ν and subsequently use Eq. (83) and Poisson identity to express the lattice sums in real space as in Eq. (84). By requiring that the resulting expressions of $\partial F/\partial\alpha$ and $\partial F/\partial\nu$ be zero, we obtain the following equations:

$$\alpha = \beta\left\{\sum_{\mathbf{R}\neq 0}\nabla^2 w(R) + \frac{\delta_{\rm eff}^2}{2}\sum_{\mathbf{R}\neq 0}\nabla^2\nabla^2 w(R) + \frac{1}{2\alpha}\sum_{\mathbf{R}\neq 0}\nabla^2\nabla^2 w(R) + \frac{\delta_{\rm eff}^2}{4\alpha}\sum_{\mathbf{R}\neq 0}\nabla^2\nabla^2\nabla^2 w(R)\right.$$
$$\left. - \frac{\delta_{\rm eff}^2}{2}\frac{I_0'\left(\frac{\beta}{v}\delta_{\rm eff}^2\lambda_{\rm eff}\right)}{I_0\left(\frac{\beta}{v}\delta_{\rm eff}^2\lambda_{\rm eff}\right)}\sum_{\mathbf{R}\neq 0}\left(\frac{\partial^2}{\partial x^2} - \frac{\partial^2}{\partial y^2}\right)\left[\nabla^2 w(R) + \frac{1}{2\alpha}\nabla^2\nabla^2 w(R)\right]\right\}, \tag{C1}$$

$$\nu = 2\beta\delta^2\left[1 + \frac{4\nu^2 + 11\nu + 6}{\nu(1+\nu)^2}\right]\left\{\sum_{\mathbf{R}\neq 0}\left[\nabla^2 w(R) + \frac{1}{2\alpha}\nabla^2\nabla^2 w(R)\right] - \frac{\lambda_{\rm eff}}{v}\frac{I_0'\left(\frac{\beta}{v}\delta_{\rm eff}^2\lambda_{\rm eff}\right)}{I_0\left(\frac{\beta}{v}\delta_{\rm eff}^2\lambda_{\rm eff}\right)}\right\} - \frac{\nu(1+2\nu)}{(1+\nu)^2}, \tag{C2}$$

with $\delta_{\rm eff}$ and $\lambda_{\rm eff}$ given, respectively, by Eqs. (80) and (85). Equations (C1) and (C2) were solved iteratively for α and ν at fixed lattice constant a. As initial guess, we took the α and ν obtained from these equations by disregarding the terms of order $1/\alpha$ and $1/\nu$.

APPENDIX D: SPECIFIC HEAT AT LOW TEMPERATURE

Here we determine the behavior of the configurational specific heat per particle at constant volume c_V at low temperature. By differentiating with respect to β the expression of $\beta F/N$ given by Eq. (84) we obtain the internal energy per particle E/N,

$$\frac{E}{N} = \mathcal{S} - \frac{1}{2v}\delta_{\rm eff}^2\lambda_{\rm eff}\frac{d}{d\psi}\ln[I_0(\psi)] + \frac{1}{2}w(0), \tag{D1}$$

where for ease of notation we have set

$$\mathcal{S} = \sum_{\mathbf{R}\neq 0} w(R) + \frac{\delta_{\rm eff}^2}{2}\sum_{\mathbf{R}\neq 0}\nabla^2 w(R)$$
$$+ \frac{1}{2\alpha}\sum_{\mathbf{R}\neq 0}\nabla^2 w(R) + \frac{\delta_{\rm eff}^2}{4\alpha}\sum_{\mathbf{R}\neq 0}\nabla^2\nabla^2 w(R), \tag{D2}$$

$$\psi = \frac{\beta}{v}\delta_{\rm eff}^2\lambda_{\rm eff}. \tag{D3}$$

We observe that Eq. (84) depends on temperature both explicitly and implicitly via the variational parameters λ, α, ν, but those parameters do not contribute to the temperature derivative of F because of the optimization conditions $\partial F/\partial\lambda = \partial F/\partial\alpha = \partial F/\partial\nu = 0$. However, they do contribute to the temperature derivative of E needed to obtain c_V, since we have

$$\frac{dE}{d\beta} = \frac{\partial E}{\partial\beta} + \frac{\partial E}{\partial\lambda}\frac{d\lambda}{d\beta} + \frac{\partial E}{\partial\alpha}\frac{d\alpha}{d\beta} + \frac{\partial E}{\partial\nu}\frac{d\nu}{d\beta}. \tag{D4}$$

We now turn to the optimization conditions on λ, α, ν. They read

$$\frac{\partial\mathcal{S}}{\partial\lambda} = \frac{1}{2v}\delta_{\rm eff}^2\frac{\partial\lambda_{\rm eff}}{\partial\lambda}\frac{d}{d\psi}\ln[I_0(\psi)], \tag{D5}$$

$$\frac{\partial\mathcal{S}}{\partial\alpha} = \frac{1}{2v}\delta_{\rm eff}^2\frac{\partial\lambda_{\rm eff}}{\partial\alpha}\frac{d}{d\psi}\ln[I_0(\psi)] - \frac{1}{\beta}\frac{\partial}{\partial\alpha}G(\alpha,\nu), \tag{D6}$$

$$\frac{\partial\mathcal{S}}{\partial\nu} = \frac{1}{2v}\lambda_{\rm eff}\frac{d\delta_{\rm eff}^2}{d\nu}\frac{d}{d\psi}\ln[I_0(\psi)] - \frac{1}{\beta}\frac{\partial}{\partial\nu}G(\alpha,\nu), \tag{D7}$$

with $G(\alpha,\nu)$ given by Eq. (77). We differentiate Eq. (D1) with respect to λ, α, ν, and express the partial derivatives of $\mathcal{S}$ via Eqs. (D5)–(D7). This gives

$$\frac{d}{d\beta}\left(\frac{E}{N}\right) = -\left[\frac{1}{v}\delta_{\rm eff}^2\lambda_{\rm eff} + \frac{\beta}{v}\delta_{\rm eff}^2\frac{\partial\lambda_{\rm eff}}{\partial\lambda}\frac{\partial\lambda}{\partial\beta}\right.$$
$$\left. + \frac{\beta}{v}\delta_{\rm eff}^2\frac{\partial\lambda_{\rm eff}}{\partial\alpha}\frac{\partial\alpha}{\partial\beta} + \frac{\beta}{v}\lambda_{\rm eff}\frac{d\delta_{\rm eff}^2}{d\nu}\frac{d\nu}{d\beta}\right]$$
$$\times\frac{1}{2v}\delta_{\rm eff}^2\lambda_{\rm eff}\frac{d^2}{d\psi^2}\ln[I_0(\psi)]$$
$$- \frac{1}{\beta}\frac{\partial}{\partial\alpha}G(\alpha,\nu)\frac{d\alpha}{d\beta} - \frac{1}{\beta}\frac{\partial}{\partial\nu}G(\alpha,\nu)\frac{d\nu}{d\beta}. \tag{D8}$$

Let us consider the low-temperature behavior of Eq. (D8): Eqs. (C1) and (C2) imply that for $\beta\to\infty$ one has $\alpha\sim\beta$, $\nu\sim\beta$, so both α and ν diverge in this limit, whereas λ tends to a finite value determined by the lattice constant at $T = 0$. From Eqs. (77), (80), (82), and (D3) we find in the same

limit

$$\lambda_{\rm eff} \to \lambda, \quad \delta_{\rm eff} \to \delta, \quad \frac{d^2}{d\psi^2} \ln\left[I_0(\psi)\right] \to \frac{1}{2\psi^2},$$
$$\frac{\partial \lambda_{\rm eff}}{\partial \lambda} \to 1, \quad \frac{\partial \lambda_{\rm eff}}{\partial \alpha} \sim \frac{1}{\alpha^2}, \quad \frac{d\delta_{\rm eff}^2}{d\nu} \sim \frac{1}{\nu^2},$$
$$\frac{\partial}{\partial \alpha} G(\alpha, \nu) = \frac{1}{2\alpha}, \quad \frac{\partial}{\partial \nu} G(\alpha, \nu) \to \frac{1}{2\nu}. \tag{D9}$$

From Eq. (D9) it is found that in the summation inside the square brackets in Eq. (D8), only the first term survives for $T \to 0$. Putting everything together we obtain

$$c_V = -k_{\rm B}\beta^2 \frac{\partial}{\partial \beta}\left(\frac{E}{N}\right) \to k_{\rm B}\left(\frac{1}{4} + \frac{1}{2} + \frac{1}{2}\right) = 1.25\, k_{\rm B}, \tag{D10}$$

corresponding to a thermal capacity per dimer

$$c_V^{\rm dimer} = 2c_V \to k_{\rm B}\left(\tfrac{1}{2} + 1 + 1\right) = 2.5\, k_{\rm B}, \tag{D11}$$

where the $k_{\rm B}/2$ contribution comes from the rotational degree of freedom, accounted for by the term containing $d^2 \ln[I_0(\psi)]/d\psi^2$ in Eq. (D8), one of the $k_{\rm B}$ contributions comes from the two degrees of freedom describing the oscillations of the dimer center of mass, accounted for by the term containing $\partial G/\partial \alpha$, and the other $k_{\rm B}$ comes from the degree of freedom determining the distance between the dimer particles, accounted for by the term containing $\partial G/\partial \nu$. The last contribution is twice that expected on the basis of equipartition of energy, as discussed in Sec. V.

[1] S. R. Nagel, Rev. Mod. Phys. **89**, 025002 (2017).
[2] C. N. Likos, A. Lang, M. Watzlawek, and H. Löwen, Phys. Rev. E **63**, 031206 (2001).
[3] B. M. Mladek, P. Charbonneau, C. N. Likos, D. Frenkel, and G. Kahl, J. Phys.: Condens. Matter **20**, 494245 (2008).
[4] B. M. Mladek, D. Gottwald, G. Kahl, M. Neumann, and C. N. Likos, Phys. Rev. Lett. **96**, 045701 (2006); **97**, 019901(E) (2006).
[5] C. N. Likos, B. M. Mladek, D. Gottwald, and G. Kahl, J. Chem. Phys. **126**, 224502 (2007).
[6] Y. Norizoe and T. Kawakatsu, Europhys. Lett. **72**, 583 (2005).
[7] M. Rey, A. D. Law, D. M. A. Buzza, and N. Vogel, J. Am. Chem. Soc. **139**, 17464 (2017).
[8] M. Rey, T. Yu, K. Bley, K. Landfester, D. M. A. Buzza, and N. Vogel, Langmuir **34**, 9990 (2018).
[9] V. S. K. Balagurusamy. G. Ungar, V. Perec, and G. Johansson, J. Am. Chem. Soc. **119**, 1539 (1997).
[10] G. A. McConnell and A. P. Gast, Phys. Rev. E **54**, 5447 (1996).
[11] G. A. McConnell and A. P. Gast, Macromolecules **30**, 435 (1997).
[12] S. Fischer and A. Exner, Proc. Natl. Acad. Sci. USA **108**, 1810 (2011).
[13] J. Fornleitner and G. Kahl, Europhys. Lett. **82**, 18001 (2008).
[14] J. Fornleitner and G. Kahl, J. Phys.: Condens. Matter **22**, 104118 (2010).
[15] G. J. Pauschenwein and G. Kahl, Soft Matter **4**, 1396 (2008).
[16] G. J. Pauschenwein and G. Kahl, J. Chem. Phys. **129**, 174107 (2008).
[17] F. Mambretti, S. Molinelli, D. Pini, G. Bertaina, and D. E. Galli, Phys. Rev. E **102**, 042134 (2020).
[18] F. Mambretti, M. Martinelli, F. Civillini, M. Bertoletti, S. Riva, N. Manini, D. E. Galli, and D. Pini, Phys. Rev. E **104**, 044602 (2021).
[19] S. Prestipino and F. Saija, J. Chem. Phys. **141**, 184502 (2014).
[20] T. Neuhaus and C. N. Likos, J. Phys.: Condens. Matter **23**, 234112 (2011).
[21] S. Prestipino, D. Gazzillo, and N. Tasinato, Phys. Rev. E **92**, 022138 (2015).
[22] A. Little, C. Lee, C. John, S. Doyle, E. Maniv, N. L. Nair, W. Chen, D. Rees, J. W. F. Venderbos, R. M. Fernandes, J. G. Analytis, and J. Orenstein, Nat. Mater. **19**, 1062 (2020).
[23] W. H. Press, S. A. Teukolsky, W. T. Vetterling, and B. P. Flannery, *Numerical Recipes*, 2nd ed. (Cambridge University Press, Cambridge, UK, 1992).
[24] N. Metropolis, A. W. Rosenbluth, M. N. Rosenbluth, A. H. Teller, and E. Teller, J. Chem. Phys. **21**, 1087 (1953).
[25] M. Rossini, L. Consonni, A. Stenco, L. Reatto, and N. Manini, Phys. Rev. E **97**, 052614 (2018).
[26] T. Rovelli, BSc Thesis, Università di Milano, 2022.
[27] E. Stiakakis, N. Jung, N. Adžić, T. Balandin, E. Kentzinger, U. Rücker, R. Biehl, J. K. G. Dhont, U. Jonas, and C. N. Likos, Nat. Commun. **12**, 7167 (2021).
[28] N. Osterman, D. Babič, I. Poberaj, J. Dobnikar, and P. Ziherl, Phys. Rev. Lett. **99**, 248301 (2007).
[29] A. Drozd-Rzoska, S. Starzonek, S. J. Rzoska, J. Łoś, Z. Kutnjak, and S. Kralj, Molecules **26**, 429 (2021).